Contents

List of Figures

List of Tables

Chapter 1

Introduction and Background

1.1 Introduction

Direction-of-arrival (DOA) estimation of the incoming signals is a basic and important technique in microphone array processing. It is applied not only for wireless communication but also for audio/speech processing systems.

A lot of applications such as hearing aids and speech recognition require the knowledge of the source localization. A adaptive spatial filter could be designed afterwards to attenuates the noise from other directions and enhance the signal from the coming direction. Therefore, a correct DOA detection becomes very important.

The classical method for DOA estimation with microphone arrays is so-called beamforming. Beamforming is nothing else but a spatial filter that steers the array to a desired direction in space [2]. The output of the beamformer is larger when a source arrives from the direction to which the array is steered. However, the conventional beamforming can not solve the sources that are spaced less than a beamwidth [3].

To resolve the problem, the well known signal subspace algorithms are introduced. The core of the algorithms is to find the signal subspace or eigenstructure by using either eigenvalue decomposition (EVD) or single value decomposition (SVD)

of the array output covariance matrix. The typical representatives are the MUSIC (Multiple Signal Classification) [4] and ESPRIT (Estimation of Signal Parameters via Rotational Invariance Techniques) [5].

The subspace algorithms are widely studied on the ULA (Uniform Linear Array). However the ULA can only provide one-dimensional angle estimation and the azimuth angle is restrict in 180°. Recently, more researches have been done on UCA (Uniform Circular Array). In stead of 180° azimuthal coverage when the ULA is applied, the UCA provides 360° azimuth detectable range.

1.2 Task Description

A speech recognition algorithm is developed on a robotic system. To successfully make the system functioning, the speech received at the robot has to be clear enough. In a noisy environment, the speech signal will be corrupted by different noise signals such as motor sound, air conditions, etc. Because of the reflection of the walls, the signal is even distorted by the reverberation signals. Therefore, it is very necessary to realize some applications that could do the job of noise reduction and dereverberation. One prior option is to design a spatial filter that could attenuate the noise signal from other direction and enhance the signal from direction of the speaker. To successfully design a spatial filter, it requires a knowledge of the direction of the signal source. Therefore, a algorithm that could correctly detect the direction-of-arrival of the speech signal is very necessary.

In the past, some algorithms are developed in ULA that could detect the azimuth angle from $-90°$ to $90°$ [6] [7]. However, the robot needs to localize the speaker from all azimuthal angle. Therefore, a Uniform Circular Array (UCA) is applied here to develop a DOA algorithm which has 360° azimuthal convergence. In the end, a hardware implementation has to be done on TI-board for the real time. Therefore, the algorithm requires faster calculation speed.

The UCA-ESPRIT algorithm is chosen to be implemented on the hardware. Unlike the normal ESPRIT and MUSIC in the ULA, the UCA-ESPRIT doesn't deal with the array output in element space. In stead, it needs to be transformed into beamspace at first. The purpose to do that is to change the steering vector in UCA to be Vandermonde like the one in ULA. In addition, the beamspace element length is less than the one in element space, which makes the calculation faster.

The classic UCA-ESPRIT algorithm can only detect the DOAs for narrowband source. The final goal is that the algorithm could localize the normal speech signal which is wideband. Two common methods, which are coherent and incoherent, will be discussed. The coherent method leads to a faster calculation speed, which is more suitable to be applied for hardware implementation.

1.3 Thesis Organization

The dissertation consists of the following chapters. In the following chapter, some fundamental concept to develop a subspace DOA algorithm is introduced. In the 3^{rd} the principle of the classic DOA algorithms (such as MUSIC, ESPRIT, UCA-RB-MUSIC, UCA-ESPRIT) is discussed. In 4^{th} chapter, the simulation for the classic DOA algorithms is presented. The performance for each algorithm is analyzed. In 5^{th} chapter, the concept of wideband DOA algorithm implementation is introduced. The simulation results will be discussed in 6^{th} chapter. In 7^{th} chapter, a real-time system, which is based on the UCA-ESPRIT, is implemented on UCA. The testing results are shown to judge the performance of the system. In 8^{th} chapter, a conclusion is made and the possible future work is discussed as well.

Chapter 2

Fundamental concept for subspace-based DOA algorithms

This thesis is focusing on the subspace DOA algorithms, which gives a high-resolution detection results. The algorithms could be applied for different microphone geometries. The widely used array geometries are either ULA or UCA. In this chapter, both microphone arrays will be introduced and the difference between each other will be discussed as well. In addition, some assumptions have to be made to successfully apply the classic DOA algorithms.

The main core of the subspace DOA algorithms is to extract from signal and noise subspace from the array output. Two common approaches (EVD and SVD) is going to be discussed in this chapter as well. The step of how to form the spatial covariance matrix before subspaces extraction is presented.

2.1 Data Model

Nowadays, all the DOA algorithms are model based. In another word, to successfully apply the classic DOA algorithms, some assumptions have to be set up. In the following, the two assumptions has to be satisfied before doing DOA estimation. (Far-field assumption and narrowband assumption)

2.1.1 Far-field Assumption

When the source radiates from a far enough position to the microphone array, the wavefront generated by the source is approximately planar. In this situation, it could be assumed that the source locates at a far-field position. A rule of thumb [8] defines that the distance between signal source and microphone array should be larger than $2D^2/\lambda$. D is the dimension of the array and λ is wavelength of the signal. Then the signal source is approximately far-field.

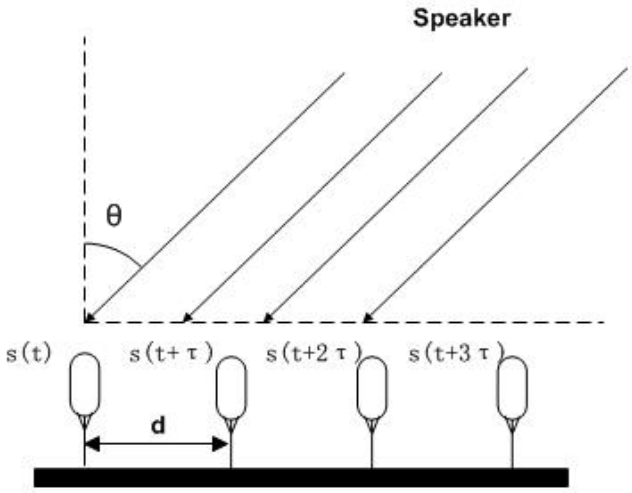

Figure 2.1: Far-field source location

Figure 2.1 shows the arriving signals with different delays. The delay between adjacent microphone is depending on the distance between the microphones and the arriving

angle, which is represented as $\tau = d \sin\theta / v$. In the equal-spaced linear array, the delay time between the signal received at 1^{st} microphone and the m^{th} microphone is then:

$$\tau_m = (m-1)\frac{d \sin\theta}{v} = (m-1)\tau \tag{2.1}$$

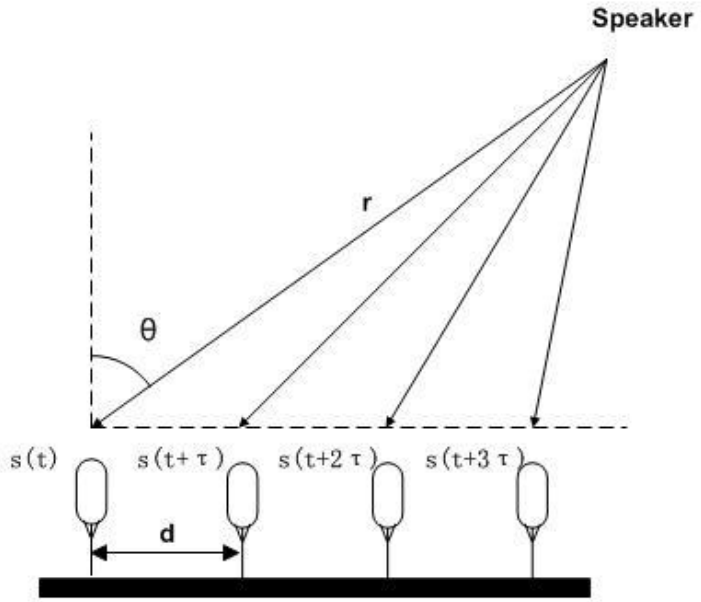

Figure 2.2: Near-field source location

When the signal source locates close to the microphone array, the time delay depends not only on d, θ, v, but also on the distance r between the speaker and the microphone array as shown in Figure 2.2. The time delays between adjacent microphones are not equal as in far-field case. It is also depending on the distance between the 1^{st} microphone and the speaker.

$$\tau_m = \frac{r - \sqrt{r^2 - 2(m-1)rd\sin\theta + ((m-1)d)^2}}{v} \tag{2.2}$$

Here the wave that impinge on each array has to be parallel to successfully develop the DOA algorithms. Therefore, the signal must locate far enough to be likely in far-field.

2.1.2 Narrowband Assumption

Besides that the signals have to locate far enough to make a planar wavefront on the microphone array, the classic DOA algorithm also requires the signal to be narrowband. Assuming that s(t) is the signal source, then the received signal at the microphone could be represented as

$$s(t) = \alpha s(t - \tau) \tag{2.3}$$

where α is the attenuation factor and τ is the delay time difference. Here, the noise is not taken into consideration. The signal that received at microphones is not distorted by the noise. In the frequency domain, the time delay directly translates to a phase shift.

$$s(r - \tau) \leftrightarrow S(f)e^{-j2\pi f\tau} \tag{2.4}$$

Assumed that the signal has centre frequency f_c, and the bandwidth is much less compare with the centre frequency.

$$f_c - \frac{B}{2} \leq f \leq f_c + \frac{B}{2} \qquad \text{when } B \ll f_c$$

Then f could be approximately equal to the centre frequency and phase-shift is approximately constant over all the bandwidth. The above equation could be rewritten as:

$$S(f)e^{-j2\pi f_c\tau} \approx S(f)e^{-j2\pi f\tau} \leftrightarrow s(t)e^{-j2\pi f_c\tau} \tag{2.5}$$

Now, the phase shift is not depending on signal frequency. Only the time delay decides the value of the phase difference. In certain array geometry, the time delay received at each microphone varies when the signal emits from different direction. In this thesis, only ULA and UCA array geometries will be considered. Then the DOA information could be extracted from the phase difference. Therefore, the narrowband approximation has to be fulfilled at first for the signal sources:

$$s(t - \tau) \approx s(t)e^{-j2\pi f_c\tau} \tag{2.6}$$

2.2 Array Constructures

In this sections, the main array constructures that used throughout this thesis will be presented, which are Uniform Linear Array (ULA) and Uniform Circular Array (UCA). A lot of work has been investigated in the ULA already. Almost all the classic DOA algorithms are implemented on this array constructure. Recently, UCA array constructure gets more and more attention, since it has some advantages compare to the ULA.

2.2.1 Uniform Linear Array (ULA)

Consider a ULA consisting of N identical and omni-directional microphones that are aligned and equal-spaced allocate on a line. The distance between the adjacent microphones is denoted as d. In the noise-free environment, the signal that impinging on the leftmost sensor from the far-field source is define as s(t). Then, the signals that impinge on the other sensors are just a delay version of the first one.

$$s_i(t) = s(t - \tau_i) \tag{2.7}$$

Where τ_i is the relative delay time between i^{th} sensor and the first one.

Figure 2.3 shows a ULA that contains N microphones and a narrowband signal source is emitting from far-field. The waves that impinge on each array is approximately parallel. The angle between the source and the line perpendicular to the ULA is determined as the directional of arrival. It is denoted as θ. Then the delay at n^{th} microphones is presented as:

$$\tau = (n-1)\frac{d\sin\theta}{v} \tag{2.8}$$

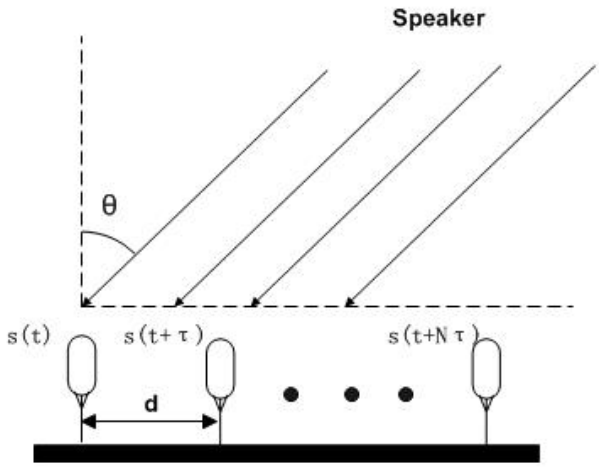

Figure 2.3: Uniform Linear Array

Spatial Aliasing

For linear array, the DOA estimation is only reliable in one side detection. In another word, the phase difference between any pair of microphone should not be more than π. The reason is that if the phase difference larger than pi, the source which gives the phase delay ϕ will be the same as the one with $2\pi - \phi$. Then it cannot tell whether the signal is coming from the front side of the microphone array or the back side. This kind of the affect is called spatial aliasing, which is not expected. To avoid the spatial aliasing, the phase difference between adjacent microphones should be restricted into π:

$$|\frac{2\pi f d \sin\theta}{v}| \leq \pi \tag{2.9}$$

The wavelength λ could replace the division between the speed and the signal frequency. The minimum wavelength is decided by the maximum frequency of the signal.

$$\lambda_{\min} = \frac{v}{f_{\max}} \tag{2.10}$$

After substitution, the above equation is written as

$$|\frac{2\pi f d \sin\theta}{v}| \leq \pi \Rightarrow d \leq \frac{\lambda}{2|\sin\theta|} \text{ and } |\sin\theta| \leq 1 \tag{2.11}$$

Considering the worst case when $\theta = 90°$, then $|\sin\theta| = 1$ and d should be less or equal than half of the wavelength. Then the maximum distance could be taken to avoid spatial aliasing is

$$d_{\max} = \frac{\lambda_{\min}}{2} \tag{2.12}$$

In reality, the distance could be adjusted according to maximum signal frequency. Normally the frequency of the speech signal is from 300Hz to 3000Hz. Suppose the maximum frequency is 4kHz, then the minimum distance between the adjacent microphones should be

$$d_{\max} = \frac{1}{2} \cdot \frac{343m/s}{4000Hz} \approx 0.043m$$

Now considering that d signal sources from different angles impinge on the ULA microphone array $s_i(t)$, $1 \leq i \leq d$, the overall signal and noise received by the m^{th} element at time t can be expressed as:

$$x_m(t) = \sum_{i=1}^{d} s_i(t - \tau_m) + n_m(t)$$

To differentiate the pure signal generated by the source and the noise-corrupted signal received at each microphone, the latter is called data and denoted by the symbol x. The steering vector is defined by collecting the phase difference of the signal at each microphone.

$$\begin{aligned} a_i(\theta) &= \begin{bmatrix} 1 & e^{-j2\pi f\tau_1} & \dots & e^{-j2\pi f\tau_N} \end{bmatrix} \\ &= \begin{bmatrix} 1 & e^{-j2\pi f\frac{d}{v}\sin\theta} & \dots & e^{-j2\pi f\frac{(N-1)d}{v}\sin\theta} \end{bmatrix} \end{aligned} \tag{2.13}$$

This equation shows the steering vector that forms the column of the steering matrix A.

$$\begin{aligned} \mathbf{A} &= \begin{bmatrix} a(\theta_1) & \dots & a(\theta_i) & \dots & a(\theta_d) \end{bmatrix} \\ &= \begin{bmatrix} 1 & \dots & 1 & \dots & 1 \\ e^{-j2\pi f\frac{d}{v}\sin\theta_1} & \dots & e^{-j2\pi f\frac{d}{v}\sin\theta_i} & \dots & e^{-j2\pi f\frac{d}{v}\sin\theta_d} \\ \dots & \dots & \dots & \dots & \dots \\ e^{-j2\pi f\frac{(N-1)d}{v}\sin\theta_1} & \dots & e^{-j2\pi f\frac{(N-1)d}{v}\sin\theta_i} & \dots & e^{-j2\pi f\frac{(N-1)d}{v}\sin\theta_d} \end{bmatrix} \end{aligned} \tag{2.14}$$

Then the data at microphone array as matrix form could be expressed as:

$$\mathbf{X} = \mathbf{AS} + \mathbf{N} \tag{2.15}$$

2.2.2 Uniform Circular Array (UCA)

In last section, the basic structure of the ULA was introduced and single ULA can only provide a $-90°$ to $90°$ angle detection. It cannot give a solution to scenarios where $360°$ of azimuth coverage and a certain degree of source elevation information are required. In these scenarios, an good alternative is to apply a circular structure, which is called Uniform Circular Array (UCA). Figure 2.4 shows an example that microphones were uniformly distributed on circumference of the UCA. The microphones are assumed to be identical and omni-directional.

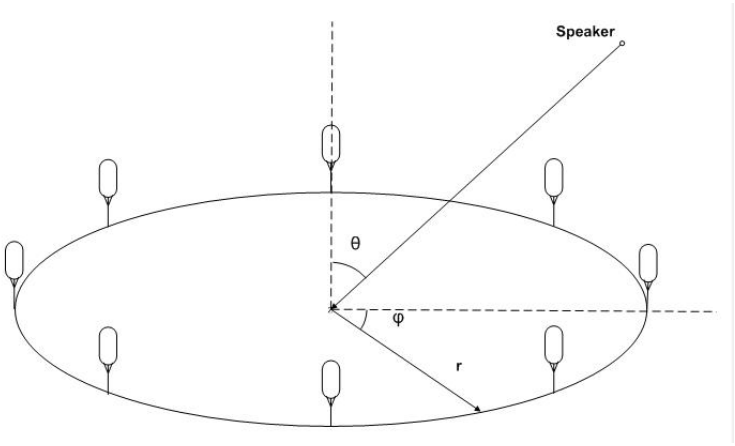

Figure 2.4: Uniform Circular Array

Consider a UCA with N sensors and radius r. If the center point of the UCA is taken as the reference point, a narrowband signal with wavelength λ arriving at n^{th} microphone from azimuth angle $\phi \in [-\pi, +\pi]$ and elevation angle $\theta \in [0, \pi/2]$ causes a phase difference, which is equal as

$$\varphi_m = kr \sin\theta \cos(\phi - 2\pi \frac{n-1}{N}), \text{ where } k = \frac{2\pi}{\lambda}$$

Here k is called wave number.Then the steering vector at n^{th} microphone could be formed as

$$a_n(\theta, \phi) = exp[jkr \sin\theta \cos(\phi - 2\pi \frac{n-1}{N})] \tag{2.16}$$

Assuming that $\zeta = kr \sin\theta$ and $\gamma = 2\pi(n-1)/N$, $n = 1, 2, \ldots, N$. The steering vector can also be written as:

$$a_n(\theta, \phi) = exp[j\zeta\theta \cos(\phi - \gamma_0), j\zeta\theta \cos(\phi - \gamma_1), \ldots, j\zeta\theta \cos(\phi - \gamma_N)] \tag{2.17}$$

The equation shows that the phase shifting at each microphone is not linear independent anymore. The steering vector is no more in Vandermonde structure. Suppose the UCA receives d narrowband signals $s_1(t), s_2(t), \ldots, s_d(t)$, the steering vector will be a $N \times d$ matrix:

$$A = \begin{bmatrix} a_1(\theta_1, \phi_1) & a_1(\theta_2, \phi_2) & \ldots & a_1(\theta_d, \phi_d) \\ a_2(\theta_1, \phi_1) & a_2(\theta_2, \phi_2) & \ldots & a_2(\theta_d, \phi_d) \\ \ldots & \ldots & \ldots & \ldots \\ a_N(\theta_1, \phi_1) & a_N(\theta_2, \phi_2) & \ldots & a_N(\theta_d, \phi_d) \end{bmatrix} \tag{2.18}$$

Comparison between ULA and UCA

After the introduction of both array constructures, two array manifolds are formed. The value of array manifold in ULA is unique when the azimuth angle is restricted between $-90°$ and $90°$. The value of the array manifold in UCA is unique when the signal is coming from the upper surface of the microphone array, which dedicates that the azimuth angle should be within $-180°$ to $180°$ and the elevation angle is restricted from 0 to $90°$. Therefore, using UCA gives a larger detectable range than using ULA.

Besides that the UCA has $360°$ detectable azimuth angle, another advantage is that it require much less space to construct UCA than ULA. To avoid spatial aliasing, the maximum distance between the adjacent microphones is 4.5cm. For a ULA which contains 8 microphones, the total length is equal to 36cm. But for a UCA that also contains also 8 microphones, the required diameter is only 9cm. Therefore, it requires

much less space to implement the algorithm on a UCA than a ULA. In practice, some hardware is very sophisticated won't leave much space to place a big array. In these situation, UCA will be a prior than ULA.

2.3 Spatial Covariance Matrix

Covariance matrix is widely used in DOA algorithms. Many DOA estimation algorithms basically extract the information from this array data covariance matrix first. It is fundamental step for the DOA estimation algorithms.

In the real world, the signals received by the array elements are noise-corrupted. Normally, the noise at each sensor is uncorrelated and the signal should be correlated since they are originated from the same source. The DOA information could be effectively extracted via this property. The spatial covariance matrix is defined as [9]

$$R_{xx} = E\{x(t)x^H(t)\} \tag{2.19}$$

The degree of the covariance matrix is up to the number of sensors. The larger the number of sensor is, the higher order of the covariance matrix will be. In practice, the exact covariance matrix of R_{xx} is difficult to find due to the limit number of the data sets. Therefore, an estimation is made by taking N samples of $x(t_n)$, $1 \leq n \leq N$. Using X to represent x(t) in matrix form, the estimation of the data covariance matrix could be calculated by the following.

$$R_{xx} \approx \hat{R}_{xx} = \frac{1}{N}\sum_{n=1}^{N} x(t_n)x^H(t_n) \tag{2.20}$$

In matrix form:

$$\hat{R}_{xx} = \frac{1}{N}\mathbf{X}\mathbf{X}^H \tag{2.21}$$

The estimated covariance matrix is used in all the classic DOA algorithms.

2.4 Subspace-based Technique

All the DOA algorithms based on subspace technique rely on the followings properties of the spatial covariance matrix R_{xx}.

- the eigenvectors of the covariance matrix could be partitioned into two spaces, which are named signal subspace and noise subspace
- the steering vector is corresponding to the signal subspace
- the signal subspace and noise subspace could be distinguished by the eigenvalues of the covariance matrix
- the spanned signal subspace is orthogonal to the spanned noise subspace

2.5 Decomposition Methods

In linear algebra, both the eigenvalue decomposition (EVD) and the singular value decomposition are (SVD) the factorization of a matrix into a canonical form. Then the matrix could be represented in terms of its eigenvalues and eigenvectors. The EVD can only be applied for the square matrix, which could be written as:

$$R = Q\Lambda Q^H = \begin{bmatrix} Q_s & Q_n \end{bmatrix} \begin{bmatrix} \Lambda_s & 0 \\ 0 & \Lambda_n \end{bmatrix} \begin{bmatrix} Q_s & Q_n \end{bmatrix}^H \tag{2.22}$$

The eigenvalues of R are listed in descending order $\lambda_1^2, \lambda_2^2, \ldots, \lambda_d^2, \ldots, \lambda_N^2$, then $\lambda_i^2 \geq \lambda_{i+1}^2$ for $i = 1, 2, \ldots, d-1$ and $\lambda_d^2 \geq \lambda_{d+1}^2 = \ldots = \lambda_N^2 = \sigma^2$. The matrix Q is partitioned into an $N \times d$ matrix Q_s whose columns are the d eigenvectors corresponding to the signal subspace, and an $N \times (N-d)$ matrix Q_n whose columns corresponding to the noise eigenvectors [10] [11] [12]. The matrix Λ is a diagonal matrix that is partitioned into two diagonal matrices (Λ_s and Λ_n). The diagonal elements of $d \times d$ Λ_s are corresponding to the signal eigenvalues. The diagonal elements of $(N-d) \times (N-d)$ Λ_n are corresponding to the noise eigenvalues, which could be written as identity matrix $\sigma^2 I_{(n-d)\times(n-d)}$. σ^2 is simply equal to the power of the noise.

An alternative decomposition method to find the eigenvectors of the spatial covariance matrix could be involved by using the data matrix X directly. This decomposition scheme is called singular value decomposition. Suppose the data matrix X contains n samples of data at N sensors. The $n \times N$ matrix X could be decomposed by SVD:

$$\mathbf{X} = \mathbf{U}\mathbf{\Sigma}\mathbf{V}^H \tag{2.23}$$

Both decomposition methods are able to extract the signal and noise subspaces. The SVD decomposition method is comparatively more stable than EVD method. For simulation and hardware implementation in later chapter, SVD is chosen as the decomposition method.

Chapter 3

Classic subspace-based DOA Methods

In this chapter, the algorithms of subspace DOA detection (MUSIC and ESPRIT) will be summarized. Both of them are the most widely used subspaces DOA estimation algorithms nowadays. A lot of work was investigated in the ULA (Uniform Circular Array) at first. Recently, people are more focusing on the DOA estimation on the UCA (Uniform Circular Array). The reason is that UCA provides 360° azimuth detectable range and the hardware requires less space.

The idea and concept of MUSIC and ESPRIT will be introduced which are normally applied for ULA. The steering vector in ULA has the Vandermonde structure. In UCA, a phase mode excitation beamforming matrix is used to make the steering vector to be Vandermonde-like. Then the DOA algorithms similar as the MUSIC and ESPRIT algorithms , which are called UCA-RB-MUSIC and UCA-ESPRIT, could be implemented.

The word 'classic' here requires that signal source should be narrowband. In addition the signal should locates far enough that the wavefront received at the microphone array is approximately planar. These two assumptions has been already discussed in the previous chapter.

3.1 MUSIC (Multiple Signal Classification)

In 1977 Schmidt exploited the measurement model in the case of sensor arrays of arbitrary form. Later he accomplished this by first deriving a complete geometric solution in the absence of noise, then cleverly extending the geometric concepts to obtain a reasonable approximate solution in the presence of noise. The resulting algorithm was called MUSIC (Multiple SIgnal Classification) and has been widely studied. [4]

Assuming the steering vector of the microphone array is **A**, then the input covariance matrix is

$$R_{xx} = AR_{ss}A^H + \sigma^2 I_N \tag{3.1}$$

where R_{ss} is the signal correlation matrix, σ_2 is the noise common variance, and I_N is the identity matrix with rank N. Suppose the eigenvalues of R_{xx} are $\{\lambda_1, \ldots, \lambda_N\}$, which leads:

$$\begin{aligned} &|R_{xx} - \lambda_i I_N| = 0 \\ &|AR_{ss}A^H + \sigma^2 I_N - \lambda_i I_N| = 0 \end{aligned} \tag{3.2}$$

Assume the eigenvalues of the $AR_{ss}A^H$ are e_i,then

$$e_i = \lambda_i - \sigma^2 \tag{3.3}$$

A is the steering vector of a microphone array which are linearly independent. It has full column rank and the signal correlation matrix R_{ss} is non-singular as long as the incident signals are not highly correlated.

When the number of incident signal d is less than the number of microphones N. The eigenvalues could determine the signal subspace and noise space. The steering vector is corresponding to the signal subspace. As discussed before, the signal subspace is orthogonal to the noise subspace. Then such a relation is formed as:

$$\underbrace{\{a(\theta_1), \ldots, a(\theta_d)\}}_{\text{steering vector}} \perp \underbrace{\{\lambda_{d+1}, \ldots, \lambda_M\}}_{\text{noise-subspace}} \tag{3.4}$$

This tells that one can estimate the signal subspace by finding the steering vectors, which are orthogonal to the $N \times d$ eigenvectors corresponding to the noise subspace. In another word, when the steering vectors lie in the signal subspace, the θ is equal to the true DOAs. Hence by through all possible array steering vectors to find those that are perpendicular to the noise space, the DOAs can be determined. Assuming P_n represents the matrix containing the noise subspace:

$$P_n = \{\lambda_{d+1}, \ldots, \lambda_N\}$$

Since the steering vectors corresponding to the signal subspace are orthogonal to the noise subspace. $a^H(\theta)P_nP_n^Ha(\theta) = 0$ for $\theta = \theta_i$ corresponding to a DOA of an incident signal. MUSIC spectrum is constructed by taking the inverse of $a^H(\theta)P_nP_n^Ha(\theta)$:

$$P_{MUSIC} = \frac{1}{a^H(\theta)P_nP_n^Ha(\theta)} \tag{3.5}$$

When there is d incident signal impinging on the microphone array, there will be d largest peaks showing in the MUSIC algorithm. The DOAs could be obtained by taking the corresponding angles that have the highest peaks.

3.2 ESPRIT

Estimation of Signal Parameters via Rotational Invariance Techniques

Although MUSIC was the first of the super-resolution algorithm to detect the DOA of the narrowband signal with additional noise, there are some limitations including the fact that the complete knowledge of the array manifold is required. That means the algorithm have to search for all the spatial space (form -90° to 90° in ULA) to get the result by applying the MUSIC algorithm for each space. Additional peak search algorithm has to be applied afterward to find DOA, which increases computation complexity. To solve the complex computation problem in the MUSIC algorithm, an algorithm called ESPRIT which is also based on signal subspace technique was introduced by Richard Roy and Thomas Kailath in 1989.

In the report of the Richard and Thomas [5], the ESPRIT retains the features of arbitrary array of sensors. But to achieve a significant reduction in computation complexity, the doublet structure of sensor array has to be fulfilled. The elements in each doublet have identical sensitivity patterns and are translationally separated by a known constant displacement vector Δ.

Using doublet structure is to separate the sensor array into two identical subarrays. In the ULA microphone array, difference choice could be done to select two subarrays. Assume the first subarray is X, the second is Y. The signal received at the i^{th} sensor on each subarray can then be express as:

$$x_i(t) = \sum_{k=1}^{d} s_k(t) a_i(\theta_k) + n_{xi}(t) \tag{3.6}$$

$$y_i(t) = \sum_{k=1}^{d} s_k(t) e^{j\omega_0 \Delta \sin\theta_k / v} a_i(\theta_k) + n_{yi}(t) \tag{3.7}$$

θ_k is the direction of arrival of the k^{th} source.
Δ is the distance between the doublet sensors.
Combining the outputs of each sensor in each subarray, the receiver data vectors could

be written as the following:

$$x(t) = As(t) + n_x(t) \tag{3.8}$$

$$y(t) = A\Phi s(t) + n_y(t) \tag{3.9}$$

$s(t)$ is the $d \times 1$ vector of impinging signals (wavefronts) that observed at the reference sensor of subarray Z_x. Φ is diagonal $d \times d$ matrix of the phase delays between the doublet sensors for the d wavefronts, could be given by

$$\Phi = diag\{e^{j\gamma_1}, \ldots, e^{j\gamma_1}\} \tag{3.10}$$

where $\gamma_d = \omega_0 \Delta \sin\theta_k / v$. Defining the total array output as z(t), which is just simply to combine the two subarray outputs, is represented by

$$z(t) = \begin{bmatrix} x(t) \\ y(t) \end{bmatrix} = \bar{A}s(t) + n_z(t) \tag{3.11}$$

where $\bar{A} = \begin{bmatrix} A \\ A\Phi \end{bmatrix}$, $n_z(t) = \begin{bmatrix} n_x(t) \\ n_y(t) \end{bmatrix}$
.

The structure of $\bar{A}$ is to imply that the diagonal matrix Φ could be obtained without the knowledge of A (steering vector). This is the main core of the ESPRIT algorithm that reduces the computation complexity compare with the MUSIC algorithm.
As the same approach of MUSIC algorithm, ESPRIT requires that N-dimensional complex vector space $\mathbf{C}^{N\times N}$ of received snapshot vectors should be separated into orthogonal subspaces (signal subspace and noise subspace) via an eigenvalue-decomposition of the covariance matrix R_{zz}.

$$R_{zz} = E[z(t)z^H(t)] = AR_{ss}A^H + \sigma^2 I \tag{3.12}$$

R_{ss} is the covariance matrix of the emitter signals, σ^2 and is the noise variance at each sensor. The covariance R_{ss} is assumed to be full rank (no unity correlated signals) and the columns of A are assumed to be linearly independent. The subarray manifold is assumed to be unambiguous (no spatial aliasing).

The eigenvalue-decomposition of R_{ZZ} has the form:

$$R_{ZZ} = \sum_{i=1}^{M} \lambda_i e_i e_i^H = E_s \Sigma_s E_s^H + \sigma^2 E_n E_n^H \tag{3.13}$$

Where the span of the d eigenvectors $E_s = \{e_1, \ldots, e_d\}$ defines the signal subspace, and $E_n = \{e_{d+1}, \ldots, e_N\}$ span the noise subspace which are the orthogonal complement of the signal subspace. All subspace techniques are based on the observation that span$\{E_s\}$ = span$\{A\}$. This implies that there exists a full rand matrix $\mathbf{T} \in \mathbf{C}^{d \times d}$, which satisfied $E_s = \mathbf{AT}$. Defining

$$\Psi = T \Phi T^{-1} \tag{3.14}$$

Then $E_s = \begin{bmatrix} E_0 \\ E_1 \end{bmatrix} = \begin{bmatrix} A \\ A\Phi \end{bmatrix} T.$

E_0 and E_1 are the signal subspaces for subarray 0 and subarray 1. The relation between the E_0 and E_1 is

$$E_1 = E_0 T^{-1} \Phi T = E_0 \Psi \tag{3.15}$$

The parameter of interest is the eigenvalues of the operator Ψ that maps E_0 onto E_1 In practice there is no operator that exactly satisfied with above formula, because both E_0 and E_1 will be estimated with errors. Therefore a total least square (TLS) is applied to estimate the operator .
A matrix was define as:

$$F = \begin{bmatrix} F_0 \\ F_1 \end{bmatrix} \in \mathbf{C}^{d \times d} \tag{3.16}$$

To minimize the $V = \left| \left[\hat{E}_0 \mid \hat{E}_1 \right] F \right|_F^2$ with $\mathbf{FF^{-1}} = \mathbf{I}$, F could be either achieved by calculate the right singular vector of $\left[\hat{E}_0 \mid \hat{E}_1 \right]$ and get the d smallest singular values, or get the d smallest eigenvalues of $\left[\hat{E}_0 \mid \hat{E}_1 \right] \left[\hat{E}_0 \mid \hat{E}_1 \right]$. After determining the F, the estimate of the operator Ψ could be done by

$$\Psi_{ES} = -F_0 F_1^{-1} \tag{3.17}$$

3.3 Phase Mode Excitation

3.3.1 Phase mode excitation in continuous circular array

In continuous circular array, the effect of inter-element spacing could be neglected. Any excitation function is periodic with period 2π and can hence be represented in terms of a Fourier series [13]. The arbitrary excitation function $\omega_m(\gamma)$ could be represented as $\omega_m(\gamma) = \sum_{m=-\infty}^{\infty} c_m e^{jm\gamma}$, where the m^{th} phase mode $\omega_m(\gamma) = e^{jm\gamma}$ is just a spatial harmonic of the array excitation, and c_m is the corresponding Fourier series coefficient. The normalized far-field pattern resulting from exciting the aperture with the m^th phase mode is $f_m^c(\theta) = \frac{1}{m}\int_0^{2\pi} \omega_m(\gamma) e^{j\zeta\cos(\phi-\gamma}d\gamma$, where the superscript c denotes the continuous aperture. Substituting for $\omega_m(\gamma)$, the far-field pattern can be expressed as:

$$f_m^c(\theta) = j^m J_m(\zeta) e^{jm\phi} \tag{3.18}$$

where $J_m(\zeta)$ is the Bessel function of the first kind of order m. The far-field pattern has the same azimuthal variation $e^{jm\phi}$ and the elevation depends on the amplitude via the Bessel function $J_m(\zeta)$. Only a limited number of modes can be excited by a given circular aperture. M is denoted as the highest excited mode. A rule of thumb for determining M is [14]:

$$M \approx k_0 r \tag{3.19}$$

M shouldn't exceed the argument ζ, because the pattern $f_m^c(\theta)$ will be quite small when the mode orders $|m| \leq M$. The beamformer for such a mode m thus severely attenuates sources from all directions.

3.3.2 Phase mode excitation in uniform circular array

Considering the phase mode excitation of an N element UCA, the normalized beamforming weight vector that excites the array with phase mode m is :

$$\begin{aligned} w_m^H &= \frac{1}{N}[e^{jm\gamma_0}, e^{jm\gamma_1}, \ldots, e^{jm\gamma_{N-1}}] \\ &= \frac{1}{N}[1, e^{j2\pi m/N}, \ldots, e^{j2\pi m(N-1)/N}] \end{aligned} \tag{3.20}$$

The array pattern $f_m^s(\theta)$ is then equal to:

$$f_m^s(\theta) = w_m^H a(\theta) = \frac{1}{N}\sum_{n=0}^{N-1} e^{jm\gamma_n} e^{j\zeta cos(\phi-\gamma_n)} \tag{3.21}$$

For mode orders$|m| < N$, the array pattern can be expressed as:

$$f_m^s(\theta) = j^m J_m(\zeta)e^{jm\phi} + \sum_{q=1}^{\infty}(j^q J_q(\zeta)e^{-jq\phi} + j^h J_h(\zeta)e^{jh\phi}) \tag{3.22}$$

where $g = Nq - m$ and $h = Nq + m$. The first term in equation is called principle term, which is identical to the far-field pattern for the continuous aperture case. The remaining terms are called residual terms, which come up due to the sampling of the continuous aperture. To make the principal term to be the dominant one, the condition $N > 2|m|$ has to be satisfied. The highest mode of the phase excitation is M, and therefore the number of microphones should be $N > 2M$. In this case, the contribution of the residual terms is small enough to be ignored. For the development of UCA-RB-MUSIC and UCA-ESPRIT algorithms, only the principal terms is taken into the consideration. The array patterns of UCA is then identical to those for the continuous circular apertures. Using the property $J_{-m}^s = (-1)^m J_m(\zeta)$ of the Bessel function, the UCA array pattern for mode m can be expressed as:

$$f_m^s(\theta) \approx j^{|m|} J_{|m|}(\zeta)e^{jm\phi} \tag{3.23}$$

With this background on phase mode excitation of UCA, it can be proceed to develop the UCA-RB-MUSIC and UCA-ESPRIT algorithms.

3.3.3 Beamforming Matrices and Manifold Vectors

Beamforming Matrices are employed to make the transformation from element space to beamspace [15]. The beamspace transformation $F^H a(\theta) = b(\theta)$ maps the UCA manifold vector $a(\theta)$ onto the beamspace manifold $b(\theta)$.
In this section three phase mode excitation based beamformer that synthesize beamspace manifolds are developed. These beamformers are denoted F_e^H, F_r^H and F_u^H. The corresponding beamspace manifolds are $a_e(\theta)$, $a_r(\theta)$ and $a_u(\theta)$. The subscripts e, r, u stand for even, real-valued and UCA-ESPRIT respectively. All three beamformers are orthogonal that satisfies $F^H F = 1$. An orthogonal matrix V is defined as

$$V = \sqrt{N}[w_{-M} \vdots \ldots \vdots w_0 \vdots \ldots \vdots w_M] \tag{3.24}$$

The vector w_m^H defined in Eq (3.20) that excites the UCA with phase mode m, leading to pattern in Eq (3.23). The factor caused by $j^{|m|}$ could be canceled by the corresponding term $j^{-|m|}$ in matrix C_v:

$$C_v = diag\{j^{-M}, \ldots, j^{-1}, j^0, j^1, \ldots, j^{-M}\} \tag{3.25}$$

Then the beamformer F_e^H is defined as

$$F_e^H = C_v V^H \tag{3.26}$$

The beamspace manifold synthesized by F_e^H is thus

$$a_e(\theta) = F_e^H(a(\theta)) \approx \sqrt{N} J(\zeta) v(\phi) \tag{3.27}$$

The azimuth variation of $a_e(\theta)$ is through the vector $v(\phi)$, which is similar to the Vandermonde form of the ULA manifold vector. The elevation information could be derived from the form of symmetric amplitude curve through the matrix of Bessel function.

$$J_\zeta = [J_M(\zeta), \ldots, J_1(\zeta), J_0(\zeta), J_1(\zeta), \ldots, J_M(\zeta)] \tag{3.28}$$

The subscript e on $a_e(\theta)$ stands for even, because the diagonal part the matrix of Bessel function are even about the centre element. The beamspace manifold vectors are centro-Hermitian, which satisfies $\tilde{I} a_e(\theta) = a_e^H(\theta)$

$\tilde{I}$ is the reverse permutation matrix:

$$\tilde{I} = \begin{bmatrix} 0 & 0 & 0 & 1 \\ 0 & 0 & 1 & 0 \\ \cdots & \cdots & \cdots & \cdots \\ 1 & 0 & 0 & 0 \end{bmatrix} \tag{3.29}$$

The matrix contains ones on the anti-diagonal and zeros elsewhere. Another Beamformer F_r^H is constructed by pre-multiply F_e^H by a matrix W^H with centro-Hermitian characteristic on rows. Multiply the space array manifold with the real-valued beamformer F_r^H will result in a real-valued beamspace manifold $b(\theta)$, which is defined as following:

$$F_r^H = W^H F_e^H = W^H C_v V^H \tag{3.30}$$

$$b(\theta) = F_r^H a(\theta) = \sqrt{N} W^H J_\zeta v(\phi) \tag{3.31}$$

Any matrix W, which satisfies $\tilde{I}W = W$, will get a real-valued beamspace manifold $b(\theta)$. Matrix W is constructed that F_r^H synthesizes the $M' = 2M+1$ beams $f(\zeta, \phi - \alpha_i)$, where $f(\zeta, \phi)$ is the basic beampattern. Here $\alpha_i = 2\pi i/M'$, $i \in \begin{bmatrix} -M & M \end{bmatrix}$ are the azimuth rotation angles. This choice of rotation angles makes W unitary, which keeps that the beamformer F_r^H has orthogonal property.

$$W = \frac{1}{\sqrt{M'}}[v(\alpha_{-M}) \vdots \ldots \vdots v(\alpha_0) \vdots \ldots \vdots v(\alpha_M)] \tag{3.32}$$

With W as above, the basic beampattern is just the sum of the components of $a_e(\theta)$, which is $f(\zeta, \theta) = \frac{N}{M'}[J_0(\zeta) + 2\sum_{m=1}^{M} J_M(\zeta)\cos(m\phi)]$. The beamformer F_r^H thus synthesizes the $M' = 2M + 1$ dimensional real-valued beamspace manifold

$$a_r(\theta) = [f(\zeta, \phi - \alpha_{-M}), \ldots, f(\zeta, \phi - \alpha_{-1}), f(\zeta, \phi), f(\zeta, \phi - \alpha_1), \ldots, f(\zeta, \phi - \alpha_M)] \tag{3.33}$$

The last beamformer F_u^H synthesizes the beamspace manifold $a_u(\theta)$ specially developed

for UCA-ESPRIT algorithm. The beamformer is defined by

$$F_u^H = C_u V^H C_u = diag\{j^M, \ldots, j^1, j^0, j^{-1}, \ldots, j^{-M}\} \tag{3.34}$$

The diagonal, unitary matrix C_u is used to eliminate the factor j^m. The result beamspace manifold is

$$a_u(\theta) = F_u^H a(\theta) \approx \sqrt{N} J_-(\zeta) v(\phi) \tag{3.35}$$

$$J_-(\zeta) = diag\{J_{-M}(\zeta), \ldots, J_{-1}(\zeta), J_0(\zeta), J_1(\zeta), \ldots, J_M(\zeta)\} \tag{3.36}$$

Compare with the beamformers F_u^H and F_r^H. The beamformer F_u^H could also be written as

$$F_u^H = C_0 W F_r^H C_0 = C_u C_e^H = diag\{(-1)^M, \ldots, (-1)^1, 1, 1, \ldots, 1\} \tag{3.37}$$

The same transformation could be done between these beamspace manifold vectors

$$a_u(\theta) = C_0 W a_r(\theta) \tag{3.38}$$

The computation of the beamspace signal subspace matrix for UCA-ESPRIT algorithm could be done via a real-valued EVD by using this property. The details could be found where the UCA-ESPRIT Algorithm was discussed.

3.4 UCA-RB-MUSIC (Real-Beamspace) Algorithm

The UCA-RB-MUSIC Algorithm employs the real-valued beamformer to transform the element space to the beamspace. The resulting beamspace data vector is $y(t) = F_r^H x(t) = A_r s(t) + F_r^H n(t)$, here A_r is vector form of $a_r(\theta)$. The corresponding beamspace covariance matrix is

$$R_y = E[y(t)y^H(t)] = BR_xB^T + \sigma I \tag{3.39}$$

where Rx is the source covariance matrix in the element space. Since the beamformer F_r^H is orthogonal, the noise in the beamspace is white sense as well. Let R denoted as the real part of the beamspace covariance matrix:

$$R = Re\{R_y\} = BRe\{R_x\}B^T + \sigma I \tag{3.40}$$

The beamspace noise and signal subspaces are calculated by applying a real-valued EVD on the real part of the beamspace covariance matrix R. Let S and G denote as the orthonormal matrices that span the beamspace signal and beamspace noise subspaces. $S = [s_1, \ldots, s_d]$ And $G = [g_{d+1}, \ldots, g_M]$ The UCA-RB-MUSIC spectrum could be calculated by

$$s_b(\theta) = \frac{1}{b_T(\theta)GG_Tb(\theta)} \tag{3.41}$$

Direction of arrivals of the sources are obtained by search d peaks in the 2D UCA-RB-MUSIC spectrum.

3.5 UCA-ESPRIT

Uniform Circular Array ESPRIT Algorithm

In the last section, the UCA-RB-MUSIC is introduced. Similar as MUSIC algorithm [4] in the ULA case, it needs to compute the UCA-RB-MUSIC spectrum over all the azimuth and elevation range, which consume a lot time. In addition, an expensive spectral peak search algorithm has to be applied to get the DOA estimation. To avoid these drawbacks that appear in the UCA-RB-MUSIC algorithm, a close-form algorithm which called UCA-ESPRIT is exploited by Cherian P. Mathews and Michael D. Zoltowski in 1994 [15], which provides automatically paired source azimuth and elevation angle estimation. The UCA-ESPRIT algorithm is fundamentally different from ESPRIT as explained in the last chapter, which is based on the identical subarrays structure. The UCA-ESPRIT is more developed via the recursive relationship between Bessel functions. However the implementation steps of the UCA-ESPRIT is similar as the ones of the normal ESPRIT algorithm applied directly in the element space. The beamformer F_u^H is the basis of the development of the UCA-ESPRIT algorithm. The corresponding beamspace manifold becomes:

$$a_u(\theta) = F_u^H a(\theta) = \sqrt{N} \begin{bmatrix} J_{-M}(\zeta)e^{-jM\phi} \\ \vdots \\ J_{-1}(\zeta)e^{-j\phi} \\ J_0(\zeta) \\ J_1(\zeta)e^{j\phi} \\ \vdots \\ J_M(\zeta)e^{jM\phi} \end{bmatrix} \tag{3.42}$$

To form the UCA-ESPRIT algorithm, three vectors with the size of $M_e = M' - 2$ are extracted from the beamspace vector, which denoted as $a^{(i)}$, $i = -1, 0, 1$. They are simply taken the first, the middle and the last M_e elements from the beamspace vector. Three transforming matrices $\Delta^{(i)}$ with $i = -1, 0, 1$ could be used to pre-multiply with $a_u(\theta)$ to form the vectors $a^{(i)}$:

$$a^{(i)} = \Delta^{(i)} a_u(\theta) \tag{3.43}$$

with

$$\Delta^{(-1)} = \begin{bmatrix} 1 & 0 & 0 & 0 & 0 & 0 \\ 0 & 1 & 0 & 0 & 0 & 0 \\ \vdots & \vdots & \ddots & \vdots & \vdots & \vdots \\ 0 & 0 & 0 & 1 & 0 & 0 \end{bmatrix} \Delta^{(0)} = \begin{bmatrix} 0 & 1 & 0 & 0 & 0 & 0 \\ 0 & 0 & 1 & 0 & 0 & 0 \\ \vdots & \vdots & \vdots & \ddots & \vdots & \vdots \\ 0 & 0 & 0 & 0 & 1 & 0 \end{bmatrix}$$

$$\Delta^{(1)} = \begin{bmatrix} 0 & 0 & 1 & 0 & 0 & 0 \\ 0 & 0 & 0 & 1 & 0 & 0 \\ \vdots & \vdots & \vdots & \vdots & \ddots & \vdots \\ 0 & 0 & 0 & 0 & 0 & 1 \end{bmatrix}$$

The property of the Bessel function, $J_{-m}(\zeta) = (-1)^m J_m(\zeta)$, leads that $a^{(1)}$ and $a^{(-1)}$ have such relationship as:

$$a^{(1)} = D\tilde{I}(a^{(-1)})^* \tag{3.44}$$

where $D = diag\{(-1)^{M-2}, \ldots, (-1)^1, (-1)^0, (-1)^1, \ldots, (-1)^M\}$.
The manifold vectors (regardless about the sign caused by the Bessel function), $a^{(0)}$ and $e^{j\phi}a^{(1)}$ are the same. Then recursive relationship of the Bessel functions is defined as following:

$$J_{m-1}(\zeta)J_{m+1}(\zeta) = (2m/\zeta)J_m(\zeta) \tag{3.45}$$

It could be applied to match the magnitude components of three vectors, which leads to:

$$\begin{aligned} \Gamma a^{(0)} &= \mu a^{(-1)} + \mu^H a^{(1)} \\ &= \mu a^{(-1)} + \mu^H D\tilde{I}(a^{(-1)})^* \end{aligned} \tag{3.46}$$

where $\mu = \sin\theta e^{j\phi}$

$$\Gamma = \frac{\lambda}{\pi r} diag\{-(M-1), \ldots, -1, 0, 1, \ldots, M-1\} \tag{3.47}$$

The partitions of the beamspace DOA matrix also satisfy the above property.

$$A_u = [a_u(\theta_1) \vdots \ldots \vdots a_u(\theta_d)] \tag{3.48}$$

Denoting $A^{(i)} = \Delta^{(i)} A_u$ with $i = -1, 0, 1$, the above equation leads to the correlation:

$$\Gamma A^{(0)} = A^{(-1)}\Phi + D\tilde{I}(a^{(-1)})^*\Phi^* \tag{3.49}$$

Where $\Phi = diag\{u_1, \ldots, u_d\} = diag\{\sin\theta_1 e^{j\phi_1}, \ldots, \sin\theta_d e^{j\phi_d}\}$.
The beamspace signal subspace matrix S_u, that spans $R(A_u)$ can be obtained without performing a complex-valued EVD. The real-valued beamformer F_r^H is employed and a real-valued EVD is performed to yield a real-valued signal subspace S that spans $R(B)$. A real-valued non-singular matrix T was introduced to get $S = BT$. The beamformer F_u^H has such relation with the real-valued beamformer F_r^H that $F_u^H = C_0 W F_r^H$. Since the matrix C_0 is unitary, thus

$$S_u = C_0 W S = C_0 W B T = A_u T \tag{3.50}$$

Applying the same partitioning method expressed above, signal subspace matrices $S^{(i)} = \Delta^{(i)} S_u$ with $i = -1, 0, 1$ are extracted from signal subspace S_u. Substituting $S^{(i)} = A^{(i)} T$, Eq. (3.49) leads to the relationship in terms of signal subspace matrices: $\Gamma S^{(0)} = S^{(-1)}\Psi + D\tilde{I}(S^{(-1)})^*\Psi^*$ where $\Psi = T^{-1}\Phi T$. Assuming $E = [S_{-1} \vdots D\tilde{I}S_{-1}^*]$ and $\Psi = \begin{bmatrix} \Psi \\ \Psi^* \end{bmatrix}$. The equation could be written in block matrix form:

$$E\Psi = \Gamma S^{(0)} \tag{3.51}$$

Under noisy condition, the matrix E and $S^{(0)}$ is replaced by the signal subspace estimations. Then the matrix $\hat{\Psi}$ that estimates Ψ could be obtained by using a least-square solution over the equation: $\hat{E}\hat{\Psi} = \Gamma S^{(0)}$. The block conjugate structure leads to a simpler LS solution. In the noise-free case, pre-multiply the matrix E^H on both left and right side of Eq. (3.51) , it becomes $E^H E\Psi = E^H \Gamma S^{(0)}$. Substituting the E according to the assumption, the system will expand as follows:

$$\begin{bmatrix} S_{-1}^H \\ S_{-1}^T D\tilde{I} \end{bmatrix} \begin{bmatrix} S_{-1} \vdots D\tilde{I}S_{-1}^* \end{bmatrix} \begin{bmatrix} \Psi_1 \\ \Psi_2 \end{bmatrix} = \begin{bmatrix} S_{-1}^H \\ S_{-1}^T D\tilde{I} \end{bmatrix} \Gamma S_0 \tag{3.52}$$

After matrix multiplication, to equate the upper and lower blocks of the above equa-

tion, the following equations have to be fulfilled:

$$\begin{aligned} S_{-1}^{H}[S_{-1}\Psi_1 + D\tilde{I}S_{-1}^{*}\Psi_2] &= S_{-1}^{H}\Gamma S_0 \\ S_{-1}^{T}[D\tilde{I}S_{-1}\Psi_1 + S_{-1}^{*}\Psi_2] &= S_{-1}^{T}D\tilde{I}\Gamma S_0 = S_{(-1)}^{T}\Gamma S_0^{*} \end{aligned} \tag{3.53}$$

To simplify the equation above, assuming d it becomes $B\Psi + C\Psi^{*} = Q$ where $\Psi = \Psi_1$, $\Psi_2 = \Psi_1^{*}$. Using subscript R and I represents the real and imaginary parts of a complex number. The following expansion is derived:

$$(B_R + jB_I)(\Psi_R + j\Psi_I) + (C_R + jC_I)(\Psi_R - j\Psi_I) = (Q_R + jQ_I) \tag{3.54}$$

Writing the equation above in matrix form, it becomes:

$$\begin{bmatrix} (B+C)_R & (C-B)_I \\ (B+C)_I & (B-C)_R \end{bmatrix} \begin{bmatrix} \Psi_R \\ \Psi_I \end{bmatrix} = \begin{bmatrix} Q_R \\ Q_I \end{bmatrix} \tag{3.55}$$

Chapter 4

Simulation for classic subspace-based DOA algorithms

In the last chapter, the basic DOA algorithms has been introduced in both ULA and UCA. In ULA, the normal MUSIC and ESPRIT could be applied. Both algorithms needs to decomposition the data outputs into two subspaces (signal subspaces and noise subspaces). The MUSIC algorithm is to find the steering vectors that are orthonormal to the noise subspaces. The ESPRIT algorithm extracts the DOA information from the diagonal matrix Ψ. Since two identical subarrays has the constant displacement Δ, the value of the matrix is only depending on the incident angles. Both algorithms are basic subspace decomposition. The difference is that the MUSIC needs information of the noise subspace and the ESPRIT needs the one of the signal subspaces.

In UCA, via phase mode excitation, difference beamforming matrices are formed to transform the steering vector from element space to beam space. Then algorithms UCA-RB-MUSIC and UCA-ESPRIT are applied to estimate the DOAs.

In this chapter, it mainly shows the simulations for all the classic DOA algorithms and analyze the performance of each algorithm by using difference parameter settings. Here the incident signal is a sinusoidal wave with given frequency, which

fulfills the assumptions discussed before. At first, some parameters are defined as:

- N: Number of microphones
- D: Number of source
- DOA: directional of arrivals
- SNR: signal-to-noise ratio

By changing one or some of them, simulation will show how these factors affect the detection result.

4.1 classic DOA algorithms in ULA

4.1.1 MUSIC

In MUSIC algorithm, the main core is find angles that make the corresponding steering vectors to be orthogonal to the noise space. The MUSIC spectrum will be calculated after scanning all the possible angle range. The DOAs is the corresponding angles that have the peak values.

Figure 4.2 and figure 4.1 shows the MUSIC spectrum for detecting signal sources from two directions. One is from 10° and the other is from 20°. The algorithm can detect the DOAs successfully in both cases, since the peaks locate at these two angles. The peak value in the spectrum with SNR = 20dB is higher than the one with 5dB. If the signal is less noise-corrupted, it will be easier to detected the DOAs.

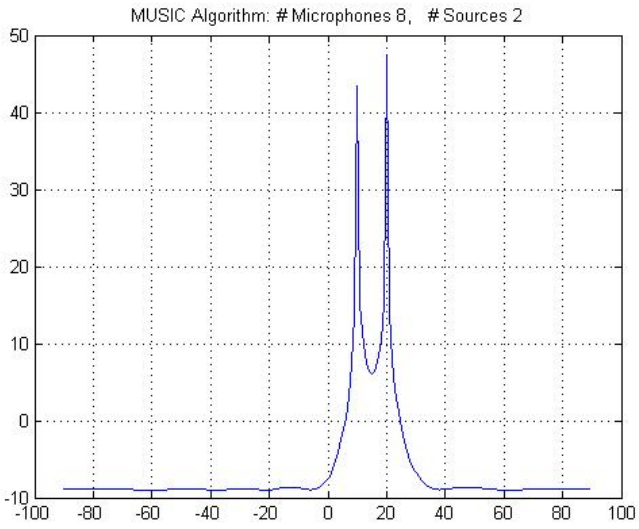

Figure 4.1: MUSIC Spectrum with SNR = 20dB

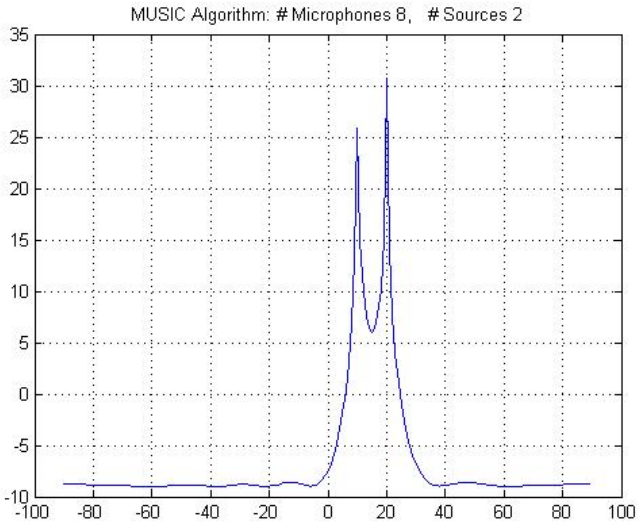

Figure 4.2: MUSIC Algorithm with SNR = 5dB

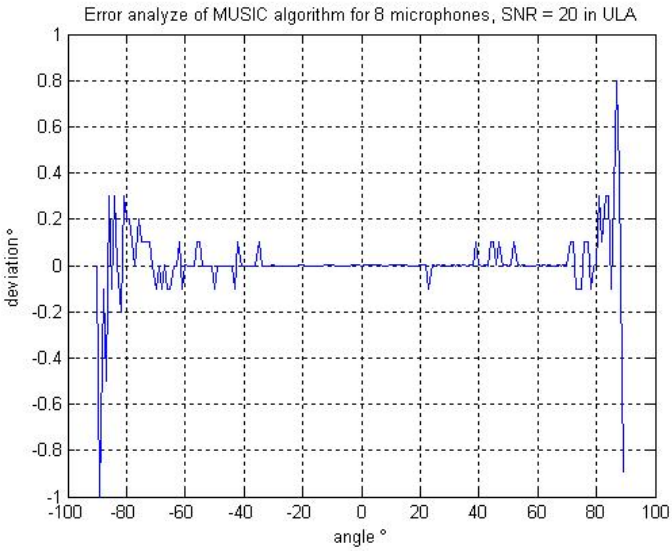

Figure 4.3: Error analyze of MUSIC algorithm with SNR = 20dB, N = 8

In MUSIC, in order to get the DOAs, the peaks search algorithms has to be implemented. The corresponding angle where the pick locates should be close to the given incident angle. Figure 4.3 shows the deviation between the given DOAs and the calculated results using MUSIC algorithm when the SNR = 20dB and number of microphone is equal to 8. The deviation is about 0.1° when the incident angle is between $-60°$ and 60°. It will increase when the incident angle is close to 90°

or $-90°$. Therefore, the MUSIC will detect the DOA successfully The accuracy is degraded when the incident angle is high.

In MUSIC algorithm, the number of the signal source should be less than the number of microphones. The noise subspace needs to be extracted from the eigen-vector of the array output. The dimension of the eigen-vector is decided by the number the microphones, which is $N \times N$. The eigen-vector contains both the signal subspace noise subspace. The first 1^{st} to d^{th} rows are the signal subspace, and $(d+1)^{th}$ to N^{th} rows are the noise subspace. When the number of source is larger or equal than the number of microphones, there is no noise subspace will be extracted. Then the MUSIC spectrum is not possible to calculate.

In the ULA, the DOAs of the signal can only be detected from one side of the microphone array. In another word, the DOAs should be given $-90°$ and $90°$. It cannot distinguish weather the signal emitting from front or the back side the microphone array.

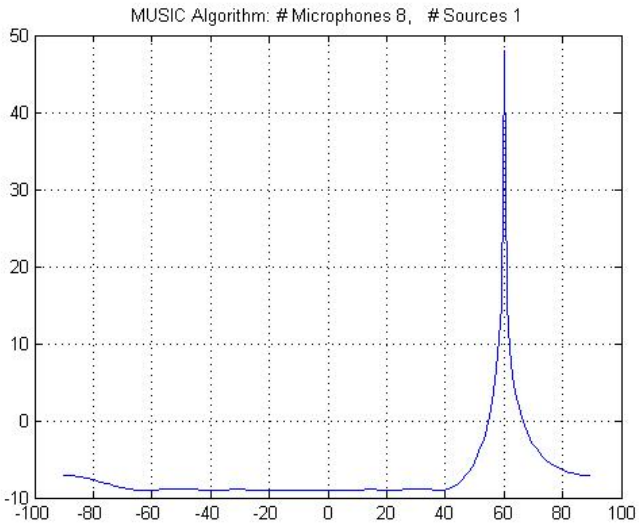

Figure 4.4: MUSIC Algorithm with $\theta = 120°$

Figure 4.4 shows the MUSIC spectrum with DOA is equal to $120°$. As it is claimed that the ULA could only detect DOA of signals from one side of the microphone

array, 120° will become 60°, which is symmetrical to the microphone array.

4.1.2 ESPRIT

ESPRIT is a close form-DOA detection algorithm. The DOAs will be given directly after calculation. No peak searching needs to be applied such as in the MUSIC algorithm. The first step of doing ESPRIT is to dividing the microphone array into two subarrays. The subarray could be either overlapped or non-overlapped. In the case of ULA with 8 microphones, the subarray could be chosen as followings.

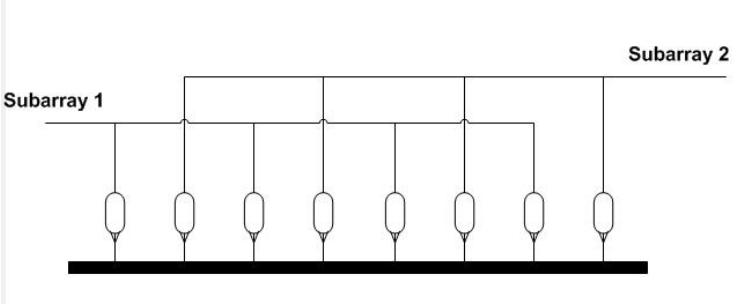

Figure 4.5: Non-overlapping subarray in ULA

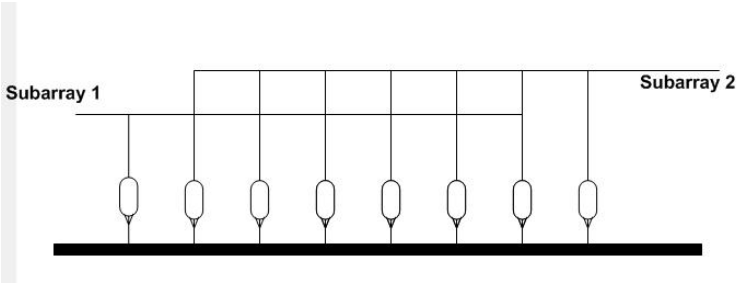

Figure 4.6: Overlapping subarray in ULA

In the non-overlapped array as figure 4.5, the 1^{st} subarray takes the odd number of the microphones and the 2^{nd} picks up the even number. For ESPRIT algorithm in ULA, the maximum number of source should be equal to the number of subarrays. In the case that the non-overlapped subarrays are selected, each array has half number

of the microphones. The maximum number of signal sources is half of the number of microphones as well.

In the overlapped case, one example is that it chooses the 1^{st} N-1 microphones as the 1^{st} subarray and from 2^{nd} to N^{th} as the 2^{nd} subarray as shown in figure 4.6. The maximum number of signal source is increased to N-1. But the trade-off is that the it take longer to calculate the eigenvector, since the length of the matrix increased as well when the SVD algorithm is applied.

Speed Analyze

overlapped subarrays	non-overlapped subarrays
N = 8, D = 1, SNR = 20dB	
0.451658s	0.304771s
N = 8, D = 2, SNR = 20dB	
0.455354s	0.301926s
N = 4, D = 1, SNR = 20dB	
0.258382s	0.219283s
N = 8, D = 1, SNR = 10dB	
0.470827s	0.338784s

Table 4.1: speed analyze for two cases of the ESPRIT in ULA

Table 4.1 shows the different calculation speed by the matlab function (tic ... toc) using ESPRIT algorithm. The measurement is done by giving different parameters. From the test, it shows the calculation speed of ESPRIT will faster by using non-overlapped subarrays than the one using overlapped. The main reason is the overlapped subarrays increase the dimension of the matrix, where a SVD algorithm needs to be calculated. ESPRIT with either overlapped subarrays or non-overlapped subarrays, the speed is only influenced by the number of microphones. The fewer the microphones are used, the faster the calculation will be.

Error Analyze

To get a better performance, the error between the given DOAs and calculated results should be as small as possible. DOA should be covering all the possible angle range ($-90°$ to $90°$).

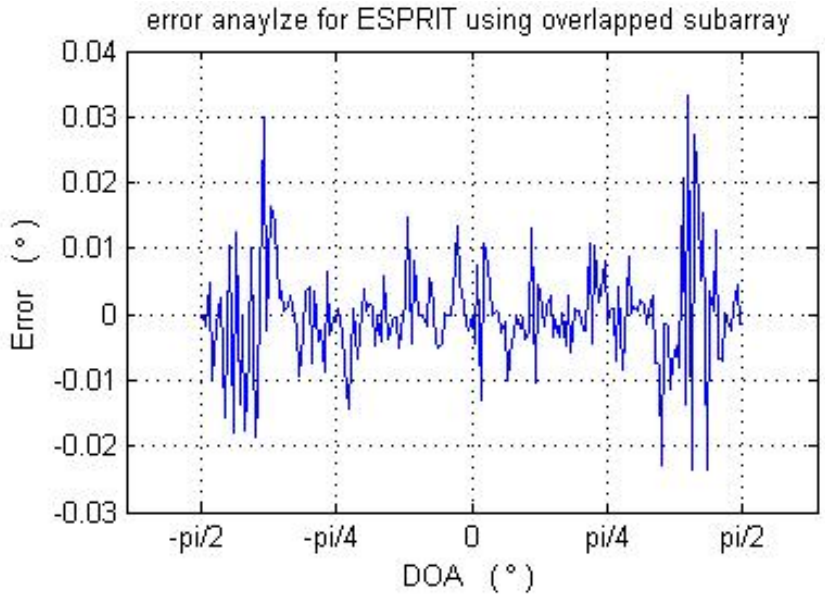

Figure 4.7: Errors for ESPRIT with overlapped subarrays

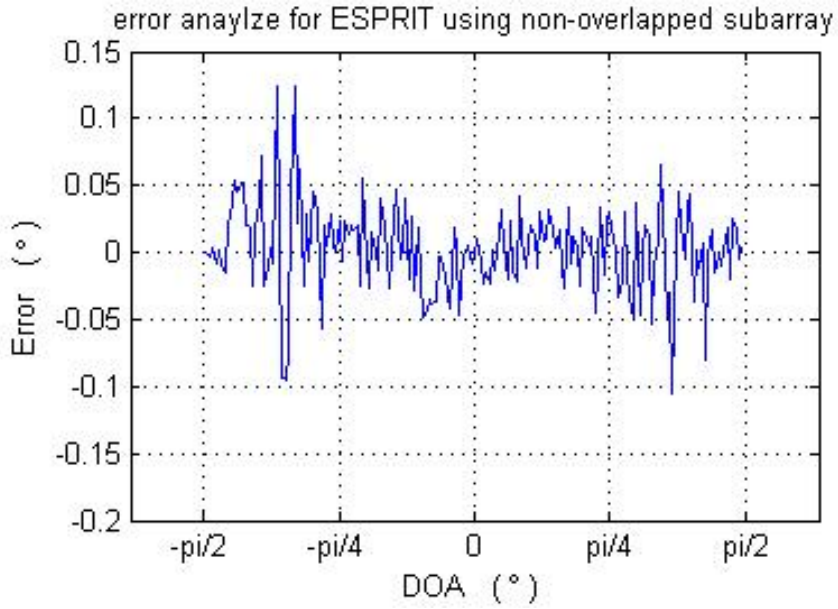

Figure 4.8: Errors for ESPRIT with non-overlapped subarrays

Figure 4.7 and figure 4.8 show the error between the real DOA and calculated result over all the detectable range. The number of microphone is equal to 8, and the SNR is fixed to 20dB. This just makes easier to compare the performance under two situations (whether the subarray is overlapped or not). The errors when the overlapped subarrays applied are much less than the errors using non-overlapped subarrays. Then it concludes that the number of microphones decides the accuracy for the DOA detecting results. The more microphones there is in the subarrays, the correctness of th results will be higher.

Above all, when an ESPRIT algorithm is applied for the DOA estimation in ULA. There is always a trade off between the speed and error deviation. Higher number of microphones in the subarray leads to a higher accuracy but a lower calculating speed and vise visa.

4.1.3 Comparison between MUSIC and ESPRIT in ULA

In the ULA, both MUSIC or ESPRIT algorithm could be applied to detect the angle of arrival. The MUSIC algorithm is to find the corresponding angles which

has the maximum value in the MUSIC spectrum. Before this step, it has to scan all the possible angle range to get the MUSIC spectrum. Both of them increase the computation load to get the DOA results. In the contrary, the ESPRIT doesn't need any searching procedure.

The deviation between the given DOAs and detect results has been analyzed for both MUSIC and ESPRIT. No matter whether overlapped subarray or non-overlapped subarray is applied for ESPRIT, the detection result using ESPRIT is more precise than MUSIC. Therefore, ESPRIT behaviors much faster and correcter comparatively. The only requirement of ESPRIT is that that the subarrays should be identical.

4.2 classic DOA algorithms in UCA

In the last chapter, the theory of doing DOA detection in UCA has been introduced. Two algorithms which so-call UCA-RB-MUSIC and UCA-ESPRIT are built based on the phase mode excitation.

4.2.1 simulation result of phase mode excitation

Phase mode excitation is to transform the element space steering vector which has the Vandermonde structure. The following shows the transformation equation:

$$f_m^s(\theta) = \frac{1}{N}\sum_{n=0}^{N-1} e^{jm\gamma_n} e^{j\zeta cos(\phi-\gamma_n)} = j^m J_m(\zeta) e^{jm\phi}$$

where $w_m^H = \frac{1}{N}[e^{jm\gamma_0}, e^{jm\gamma_1}, \ldots, e^{jm\gamma_{N-1}}]$
To prove that the beamformer w_m^H leads to the result as $j^m J_m(\zeta)e^{jm\phi}$, the test case is made as followings:

- $N = 8$, number of microphones
- $M = 5$, maximum phase mode

- $phi = 60 \cdot pi/180$, azimuth angle
- $theta = 45 \cdot pi/180$, elevation angle
- $f = 1000$, signal frequency
- $v = 343$, speech speed
- $r = 0.045$, radius of the array

$w_m^H a(\theta)$	$j^m J_m(\zeta) e^{jm\phi}$	$w_m^H a(\theta) - j^m J_m(\zeta) e^{jm\phi}$
$-0.0000 + 0.0040i$	$-0.0000 + 0.0000i$	$0.0000 - 0.0040i$
$-0.0003 - 0.0000i$	$-0.0001 + 0.0003i$	$0.0001 + 0.0003i$
$0.0000 + 0.0040i$	$-0.0000 + 0.0000i$	$-0.0000 - 0.0000i$
$0.0206 + 0.0357i$	$0.0206 + 0.0357i$	$0.0000 + 0.0000i$
$0.2418 + 0.1396i$	$0.2418 + 0.1396i$	$-0.0000 + 0.0000i$
$0.9168 - 0.0000i$	0.9168	$0.0000 + 0.0000i$
$-0.2418 + 0.1396i$	$-0.2418 + 0.1396i$	$0.0000 + 0.0000i$
$0.0206 - 0.0357i$	$0.0206 - 0.0357i$	$0.0000 + 0.0000i$
$-0.0000 + 0.0040i$	$0.0000 + 0.0040i$	$0.0000 + 0.0000i$
$-0.0003 + 0.0000i$	$-0.0001 - 0.0003i$	$0.0001 - 0.0003i$
$0.0000 + 0.0040i$	$0.0000 + 0.0000i$	$-0.0000 - 0.0040i$

Table 4.2: phase mode excitation

Table 4.2 shows the calculation results of the steering vector from element space to beamspace with phase mode $M = 5$. When $M > 3$, the beamspace steering vector won't be identical to the one at element space. To transform the steering vector in beamspace with little bias, the maximum phase mode M should be restricted in kr.

4.2.2 UCA-RB-MUSIC

Similar as calculate the noise subspace in the normal MUSIC algorithm in ULA, the UCA-RB-MUSIC algorithm is firstly to calculate the noise subspace in beamspace. Then the beamspace noise subspace is used to calculate the UCA-RB-MUSIC spectrum. The above settings are used again here, but the maximum phase mode is changed to 3. Then the expected peak of the spectrum should locate at the $\theta = 45°$,

and $\phi = 60°$.

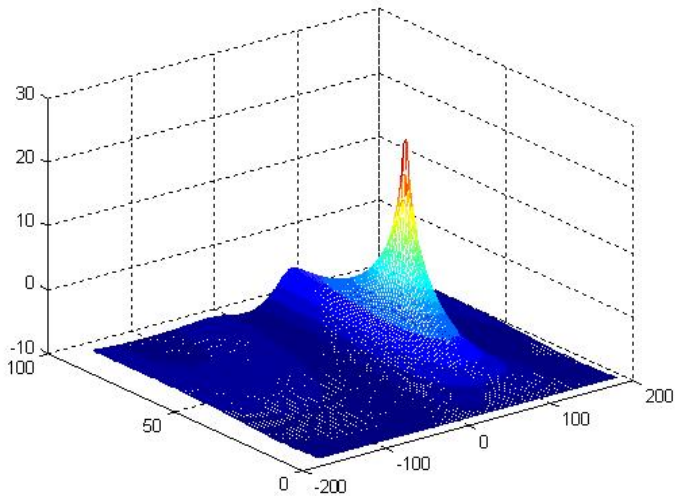

Figure 4.9: 3D plot of UCA-RB-MUSIC spectrum with $\theta = 45°$, $\phi = 60°$

Figure 4.9 shows the UCA-RB-MUSIC algorithm in 3D plot. The plot shows one peak value. To notice the corresponding elevation and azimuth angle of the peak easily, another contour plot is made.

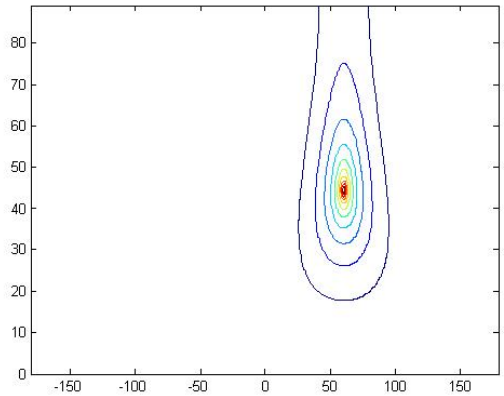

Figure 4.10: contour plot of UCA-RB-MUSIC spectrum

From the figure 4.10, the peak approximately locates at the point where $\theta = 45°$, and

$\phi = 60°$. This proves that the algorithm could detect DOA successfully.

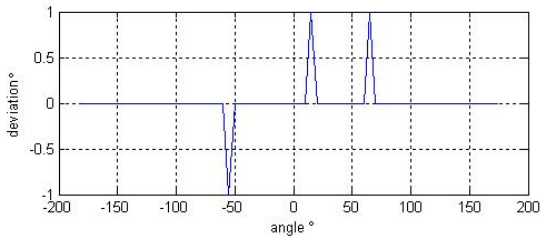

Figure 4.11: Error analyze of azimuth angle for UCA-RB-MUSIC when $\theta = 45°$

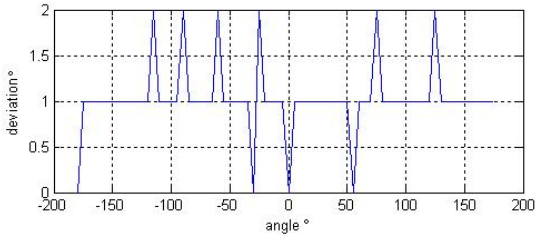

Figure 4.12: Error analyze of elevation angle for UCA-RB-MUSIC when $\theta = 45°$

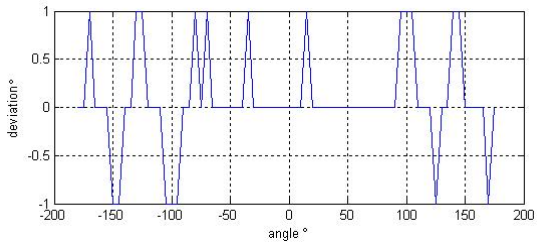

Figure 4.13: Error analyze of azimuth angle for UCA-RB-MUSIC when $\theta = 80°$

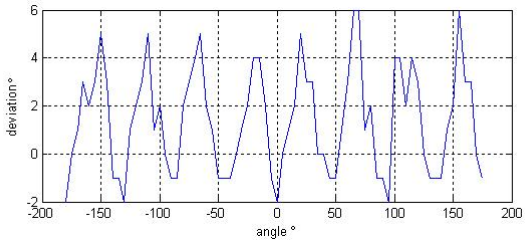

Figure 4.14: Error analyze of elevation angle for UCA-RB-MUSIC when $\theta = 80°$

Figure 4.11 - figure 4.14 shows the deviations of azimuth and elevation angles when $\theta = 45°$ and $\theta = 80°$. The results shows the UCA-RB-MUSIC algorithm could detect the azimuth angle correctly. The deviation of elevation angle gets increased when the given elevation angle changes from $\theta = 45°$ to $\theta = 80°$.

4.2.3 UCA-ESPRIT

Like ESPRIT in the ULA, the UCA-ESPRIT is also a close-form DOA detection algorithm, which gives the DOAs directly after calculation. Normally the detection results are depending on the following parameters:

- number of microphones (N)
- signal-to-noise ratio (SNR)
- elevation angle (θ)
- azimuth angle(ϕ)

The main objective is to detect the azimuthal angle correctly. Therefore, the azimuthal angle is calculated throughout all the detectable range, which is from $-180°$ to $179°$. The detected azimuth angle should be close to the expected value. The deviations are calculated by subtraction between the calculated results and the expected values to judge the performance of the algorithm in the different conditions when the other parameters vary.

Figure 4.15 shows the simulation results of the UCA-ESPIRT when the number of microphone is 8, signal-to-noise ratio is 20dB, and initial elevation angle is $45°$. The average azimuthal deviation is about $1°$, and the average deviation for elevation angle is $5°$. The result of azimuth angle is accurate compare to the elevation angle.

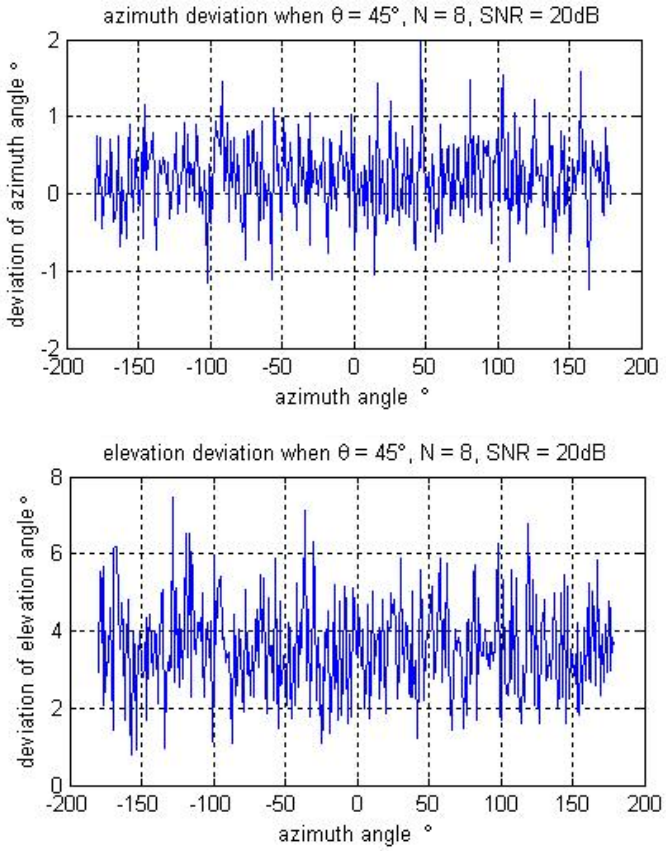

Figure 4.15: simulation of UCA-ESPRIT 1

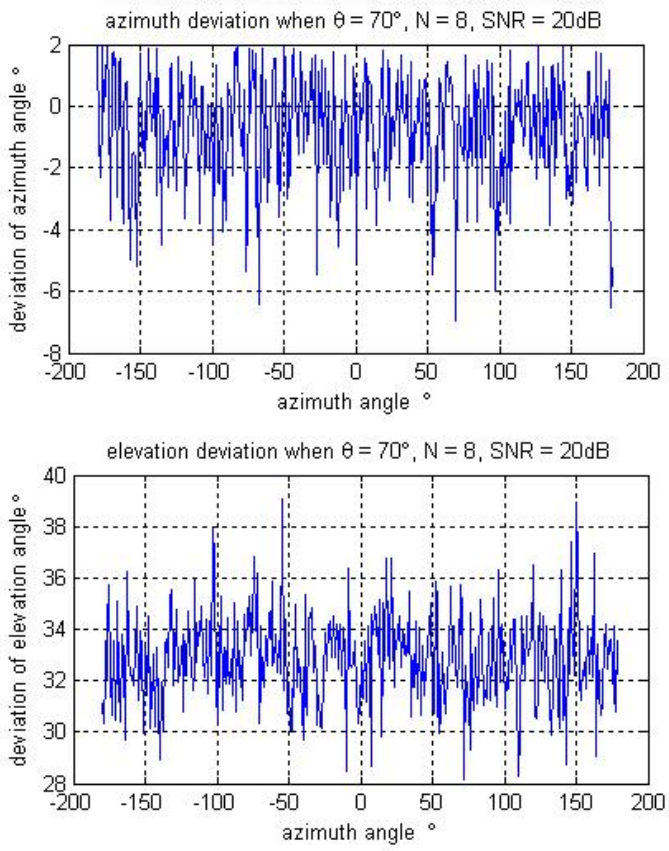

Figure 4.16: simulation of UCA-ESPRIT 2

When the elevation angle is increased to 70°, the simulation result is shown in figure 4.16. The average azimuthal deviation now increases, which is about 2°. And the average elevational deviation is about 30°. The results tell that when the azimuth angle is close to 90°, the accuracy of the UCA-ESPRIT algorithm will be degraded. Even that, the deviation of azimuth angle is still not much high, but the elevation detection is absolutely failed.

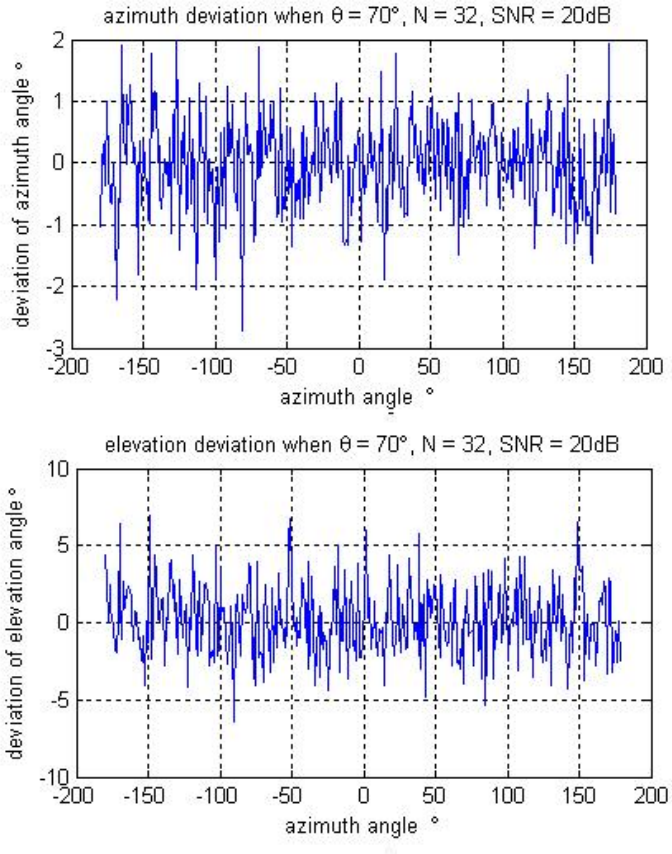

Figure 4.17: simulation of UCA-ESPRIT 3

Figure 4.17 shows the simulation result when the number of microphone is increased to 32. The accuracy of the elevation angle is becoming more precise. Here with the increment of the number of microphones, the maximum phase mode (M) increases as well. In the condition that number of microphone is 8, the maximum phase mode is equal to 8. Here the maximum phase mode is chosen as 7.

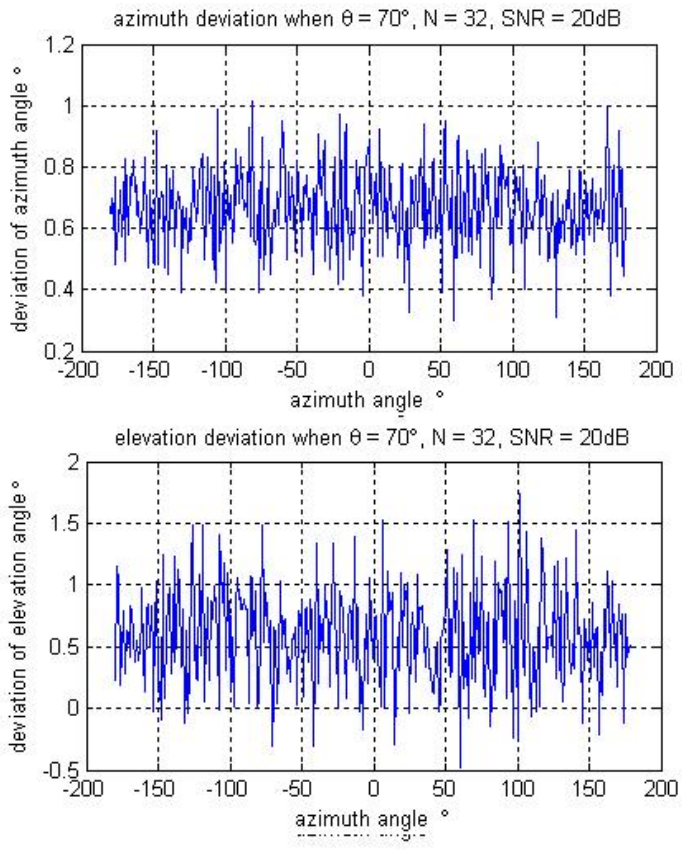

Figure 4.18: simulation of UCA-ESPRIT 4

When number of microphones is equal to 32, according to the equation introduced in the previous chapter, the maximum phase mode is 15. Figure 4.18 shows the simulation results when the maximum phase mode is set to 15. The detected azimuth and elevation angles are becoming more accurate.

In figure 4.19, the signal-to-noise ratio is changed to 5dB, which means the signal will be more corrupted by the noise. Compare with simulation result in figure 4.15, the simulation results are more accurate in the condition that SNR is high.

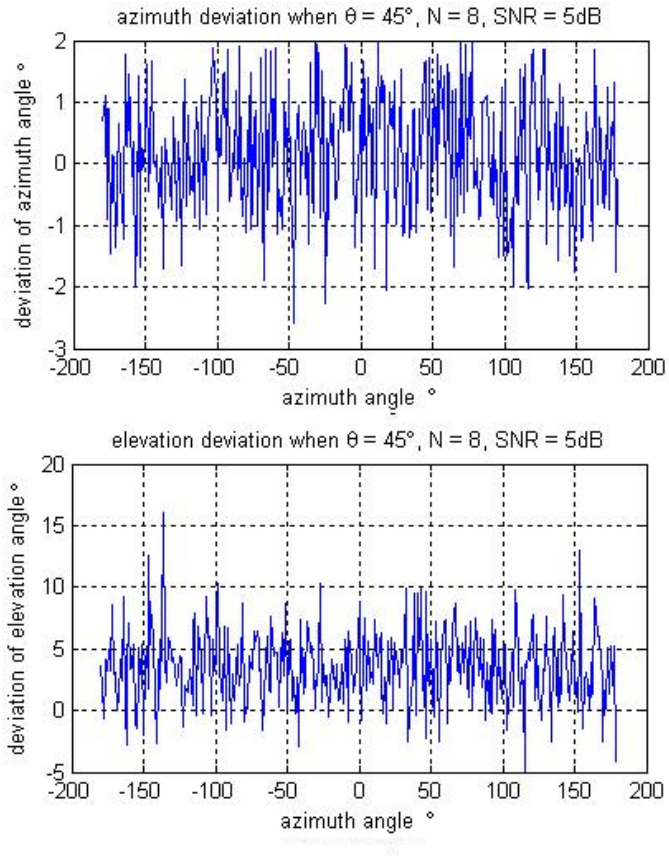

Figure 4.19: simulation of UCA-ESPRIT 5

Above all, different situations have been considered. When the elevation angle is close to 90°, the calculated elevation is not accurate but the azimuth is still close to the real DOA. To improve the elevation detection, one method is to increase the number of microphones. However, the speed of calculated will slow down. For the final implementation, the main concern is to get the right azimuth angle. Therefore, the error that occurs in the elevation could be neglected.

All the tests are done to detect the azimuth angle from $-179°$ to $180°$. The deviation between the calculated value and expected one are small. This proves that

UCA-ESPRIT can detect the azimuth angle successfully in all the situations.

4.2.4 Comparison between UCA-RB-MUSIC and UCA-ESPRIT

Both UCA-RB-MUSIC and UCA-ESPRIT are doing the DOA detection via applying a beamformer to transform the array output to beamspace. Like the MUSIC algorithm in ULA, the UCA-RB-MUSIC needs to calculate the spectrum so that the DOA could be found by searching the location of the peaks. The UCA-ESPRIT is also a close-form DOA detection algorithm like the ESPRIT in ULA. Avoiding calculating the spectrum and doing peak search, the UCA-ESPRIT is much faster compare to the UCA-RB-MUSIC.

4.3 Conclusion

In the ULA, the normal ESPRIT algorithm is applied. The microphone arrays need to divided into two identical subarray and calculate the rotational transforming matrix. In UCA, there is no subarray need to separate. In stead, the the signal subspace vector need to be partitioned into three sub-vectors. Applying the special characteristic of the Bessel function, the azimuth and elevation could be calculated directly.

From the simulation results, the UCA-ESPRIT won't give a correct elevation angle when it is close to 90°. When the number of microphone increases, the results could be improved. The trade-off is that it takes more time to calculate and more hardware requirement. Regardless of the elevation, the detection results for the azimuth angle are quite precise with limited number of microphones. Since the correct detection for the azimuth angle is the main objective, the UCA-ESPRIT could be still applied for small number of microphones.

Chapter 5

Wideband DOA Subspace-based Algorithms

In the previous chapters, the classic DOA algorithms for both ULA and UCA were introduced. As mentioned before, these algorithms can only estimate the DOA of the narrowband sources. The final goal of the implementation is that the system could detect the DOA for normal speech signals. The speech signal is wideband, which normally allocates at the frequency band between 300Hz to 3500Hz. Since the frequency is not narrowband anymore, the classic DOA method cannot directly applied.

In the previous chapter, it has been proven that only when the bandwidth is much lower than the centre frequency, it assumes that the signal is narrowband. Then the phase delay is simply a function of the delay time τ, which only depends on the DOA and array geometry. Then the DOA information could be extracted by applying a classic DOA algorithm when a ULA or a UCA is used.

When the signal source is not narrowband anymore, the phase difference doesn't rely on the location of source, but also the frequency. To successfully detect the wideband signal, one approach is done by split the whole band into certain amount bins. Then the narrownband DOA method could be calculated in each frequency

bin. This method is called incoherent. Another approach is to transform the steering vector from all frequency bins to one. The translated steering vectors are summed up to form a coherent covariance matrix. Then any narrowband algorithm could be applied for the coherent covariance matrix at the reference frequency. This class of the wideband DOA detection is named coherent. In following sections, these two main categories of the wideband DOA algorithms will be discussed.

5.1 Incoherent Wideband DOA Algorithm

The incoherent wideband DOA algorithm is to apply the narrowband DOA algorithm on all the frequency bins and average them [18] [19]. For example, when MUSIC algorithm is used as the narrowband DOA algorithm, the spectrum at K frequency bins will be sum up incoherently:

$$S_M = \frac{1}{\sum_{i=0}^{K} a^H(f_i,\theta) W_i W_i^H a(f_i,\theta)} \tag{5.1}$$

F_i: The centre frequency on each frequency bin.
W_i: The estimated noise subspace by applying the MUSIC on the array outputs at each frequency bin.
K: total number of the frequency bins

The estimated DOA could be found by using a peak search method as normal MUSIC DOA algorithm does. The corresponding angle at the peak value is the estimated DOA. The normal structure for the incoherent wideband DOA algorithm is shown in the figure 5.1.

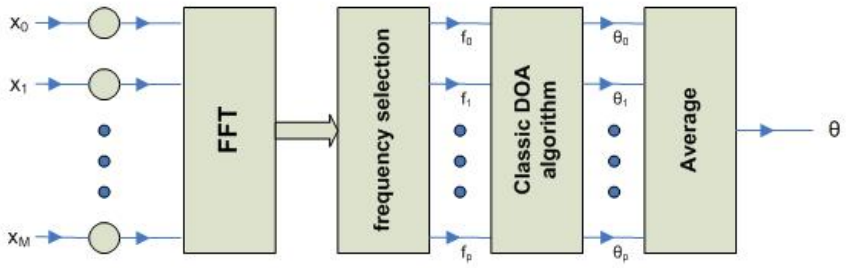

Figure 5.1: Incoherent Wideband DOA algorithm

The incoherent wideband DOA algorithm provides a good DOA estimation when the SNR is high and the noise uniformly locates at each frequency bin. In addition, the computation complexity is depending on the number of the frequency bins. The more the frequency bins there are, the more complex the computation will be, because each frequency bins need to perform a MUSIC algorithm once.

To reduce the computation load, it is better to choose certain amount of the frequency bins than to select all. A FFT (Fast Fourier Transform) algorithm could be applied to calculate the signal spectrum. Then split the spectrum into different section and select the one with maximum magnitude. After that, the narrowband DOA algorithms such as MUSIC, ROOT-MUSIC, ESPRIT, could be used on these selected frequencies. In the end, the result is taken by averaging the values calculated at each frequency.

5.2 Coherent Wideband DOA Algorithm

To avoid performing narrowband algorithm on each frequency bins, the coherent wideband DOA algorithms was introduced. The idea of the coherent wideband DOA algorithm is to align all the covariance matrices at different frequency bins into one certain frequency. Then, a narrowband DOA algorithm could be performed only once for the coherent covariance matrix. Figure 5.2 shows the structure of the coherent wideband DOA algorithm. The narrowband algorithm shown in the figure use ESPRIT.

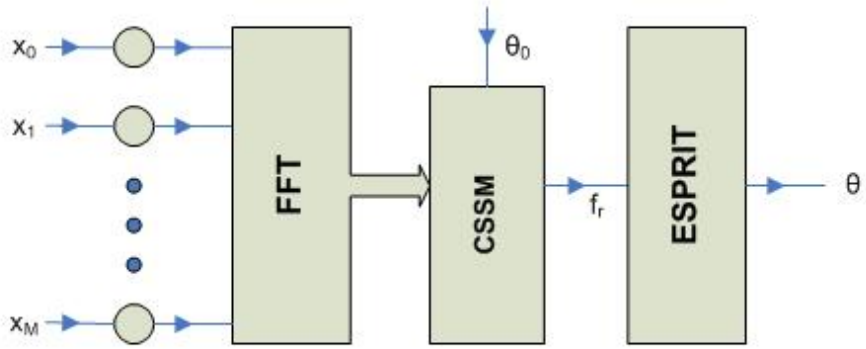

Figure 5.2: Coherent Wideband DOA algorithm

The main task for coherent wideband DOA algorithm is to align the signal subspace from all the frequency bins into one. The alignment is accomplished by a transformation of a covariance matrix on each frequency bins. After transformation, both signal and noise subspaces become coherent over the frequency bin. Then any narrowband DOA algorithm could be applied on the coherent covariance matrix to calculate DOA.

5.2.1 Coherent Signal Subspace Method (CSSM)

CSSM was introduced by Wang and Kaveh [20]. In this method, an estimation of the synthesized covariance matrix is formed via:

$$R_{com} = \sum_{i=kl}^{ku} \alpha_i T_i R_i T_i^H \tag{5.2}$$

where α_i is the weighting factors, kl and ku are respectively the inferior and superior limit. T_i is the focusing matrix for frequency f_i, which could be derived by calculating the following minimizing function.

$$\min_{T_i} \| A(f_r, \theta_r) - T_i A(f_i, \theta_i) \| \tag{5.3}$$

f_r is the reference frequency and θ_r is the focusing angles. The reference frequency could be randomly chosen in frequency band. To simplifying the R_{com} , the weighting factor is assumed to be 1 over all the frequency bins.

$$\begin{aligned} R_{com} &= \sum_{i=0}^{K} T_i R_i T_i^H \\ &= \sum_{i=0}^{K} Ti\{A(f_i,\theta_f)R_s(f_i)A^H(f_i,\theta_f) + \sigma^2(f_i)\}T_i^H \\ &\approx A(f_i,\theta_f)\sum_{i=0}^{K} R_s(f_i)A(f_r,\theta_f) + \sigma^2(f_i)T_iT_i^H \end{aligned} \tag{5.4}$$

From the equation above, it shows that the CSSM tried to composite all the transformed covariance matrices from all the frequency bins into one. The focusing matrix Ti transforms the covariance at current frequency to the reference one. The ratio between the SNR after transformation and the SNR before focusing is denoted as focusing loss.

$$g = \frac{tr\{R_n^{-1}\sum_{i=0}^{K-1} T_iA(f_i,\theta)R_sA^H(f_i,\theta)T_i^H\}}{tr\{\sum_{i=0}^{K-1} A(f_i,\theta)R_s(f_i,\theta)A^H(f_i,\theta)\}} \tag{5.5}$$

where R_n is related to the noise covariance matrix after focusing via:

$$R_n = \frac{\sum_{i=0}^{K-1}\sigma^2(f_i)T_iT_i^H}{\sum_{i=0}^{K-1}\sigma^2(f_i)} \tag{5.6}$$

The focusing loss will reach the maximum value (g=1) when the $T_iT_i^H = I$ over all the frequency bins. Assuming the focusing angle θ_r is determined, the focusing matrix T_i is found via

$$\min_{T_i} \|A(f_r,\theta_f) - T_iA(f_i,\theta_f)\|_F \tag{5.7}$$

For $i = ku \dots kl$ subject to $T_i T_i^H = I$. The solution for the above minimization problem is

$$T_i = V_i U_i^H \tag{5.8}$$

U_i and V_i are respectively the right and left singular matrices of

$$A(f_r, \theta_f) A^H(f_i, \theta_f) \tag{5.9}$$

The CSSM is robust against low SNR and has high resolution compare with incoherent method. But the performance is also decided by the focusing angle. To form the focusing matrix, a preliminary initial estimation angle has to be given. The errors in the focusing angle cause bias in the DOA estimation. How to get a good initial estimation of the DOA is a crucial question. In some documentation, it mentions that a conventional beamformer such as Capon beamformer could be applied to get the initial estimation of the DOA.

However, the conventional beamformer sometimes doesn't promise to give an accurate initial DOA estimation. Therefore, people are looking for some algorithms that don't need any preliminary angle.

5.2.2 Robust auto-focusing Coherent Signal-subspace Method (R-CSM)

In the previous section, the coherent wideband DOA estimation is analyzed. The conclusion is that the result is affected by the accuracy of the initial DOA estimation (sometimes called focusing angle). In another word, in order to improve the coherent wideband DOA estimation, the very first DOA estimation must be as accurate as possible with a low computation cost. The proposal could be either to perform narrowband DOA estimation or to use a conventional beamformer. Then, the result could be optimized by doing CSSM iteratively to reduce the estimation error. But it is not so effective since the focusing angle is still different from the actually one. To avoid this, in this section, a new method,so-called R-CSM (Robust auto-focusing Coherent Signal-subspace Method) [21], which doesn't need the initial DOA estimation is discussed.

In R-CSM, the focusing matrices required in the very first step are calculated to the following optimization problem.

$$T_k[0] = arg\{\min_{T_i} \int_{\frac{\pi}{2}}^{\frac{\pi}{2}} \|Ta(\theta, f_k) - a(\theta, f_r)\|_F^2 d\theta\} \tag{5.10}$$

where $a(\theta, f_k)$ is the array manifold evaluated at the frequency f_k. f_r is the reference frequency, θ is the focusing angle, here $\theta \in [-\frac{\pi}{2} \quad \frac{\pi}{2}]$ in the ULA case.

As it can be observed, the focusing matrix is not calculated by a given initial DOA estimation. In stead, it becomes a minimization problem with respect to the whole possible region. In the ULA, the detectable angle is from $-89°$ to $90°$. The minimization problem could be solved by least square method. The solution to the problem is given by

$$T_k[0] = V_k U_k^H \tag{5.11}$$

where U_k and V_k are respectively the right and left matrices obtained from the singular value decomposition of the matrix

$$Q_k \triangleq \int_{\frac{\pi}{2}}^{\frac{\pi}{2}} a(\theta, f_k) a^H(\theta, f_r) d\theta = U_k \Sigma V_k^H \tag{5.12}$$

After running a signal-subspace-based DOA estimation algorithm such as MUSIC, ESPRIT, a set of possibly reliable initial estimates $\hat{\theta}[0] \triangleq [\hat{\theta}_1[0], \hat{\theta}_2[0], \ldots, \hat{\theta}_d[0]]$ is available for refinement by subsequent iterations. The new focusing matrix needs to be firstly calculated by solving

$$T_k[i] = arg\{\min_{T_i} \sum_{l=1}^{d} \int_{\theta_l - \Delta_i}^{\theta_l + \Delta_i} \|T_k[i] a(\theta, f_k) - a(\theta, f_r)\|_F^2 d\theta\} \tag{5.13}$$

where $[\theta_l - \Delta_i \quad \theta_l + \Delta_i]$, $i \in 1, 2, \ldots$, refers to the new robustness intervals.

Robustness interval defines the region over which the robustness against DOA estimation errors needs to be mainly concentrated. After first iteration, it is no longer necessary to focus the array manifold over the whole visible region. It is more effective

to concentrate the spatial space around the initial DOA estimation. It makes more sense to reduce the robustness boundary after each iteration. One of the possibilities to realize the reduction of the boundaries is exponential, which obey the following rule:

$$\hat{\theta}[i] = [\max\{-\frac{\pi}{2}, \hat{\theta}_l - \frac{\pi}{2^i}\}, \min\{\frac{\pi}{2}, \hat{\theta}_u + \frac{\pi}{2^i}\}] \tag{5.14}$$

$\hat{\theta}_l$, $\hat{\theta}_u$ are respectively the largest and smallest DOA estimation from $(i-1)_{th}$ iteration.

5.2.3 Beamspace Coherent Signal Subspace Method in UCA

In the UCA, the steering vector in the element space needs to be transformed to the beamspace via phase mode excitation.

$$f_m^s(\theta) \approx j^m J_m(\zeta) e^{jm\phi} \tag{5.15}$$

The beamspace steering vector has the same phase shift which depends on the azimuth angle. The amplitude of each element is the Bessel function which depends on both the elevation and frequency. To form a matrix that could transform the beamspace steering vector from one frequency to the reference frequency, the only part need to be considered is the Bessel function.

To make the Bessel function depends only on the frequency, the elevation angle needs to be pre-defined. Normally, the speaker stays quite far from the UCA, which leads the elevation is approximately equal to 90°. Then the focusing matrix in the beamspace could be calculated as:

$$B_m = J_m(\zeta_0)/J_m(\zeta) \tag{5.16}$$

where $\zeta_0 = k_0 r$ and $\zeta = kr$.

As introduced before, a beamformer F is used to transform the steering vector from element space to beamspace. After the focusing the steering vectors from other frequencies to the reference frequency, the beamspace steering vector needs to be

transform back to element space by pre-multiply the inverse matrix of F. Therefore, an new matrix T_i could be form as such way that transform the element-space steering vector directly from one frequency to the reference one:

$$T_i = F^{-1} B_m F \tag{5.17}$$

The CSSM in UCA is not like the CSSM in ULA that could achieve the focusing loss ratio equal to 1. Therefore, the SNR before and after focusing are not identical.

Chapter 6

Simulation for Wideband Subspace-based DOA Algorithms

In the last chapter, the concept of how to implement the wideband DOA algorithms has been introduced. There are main two categories to realized the DOA detection for wideband signals. One is incoherent, which needs to applied the narrowband algorithms several times. The other is coherent, which needs the narrowband methods only once. Both methods needs to separate the signal spectrum into sections. The purpose is to treat each section as narrowband.

In this chapter, the simulation will be presentation to show the performance of the wideband DOA algorithms. An artificial signal has to be created firstly for the microphone array output via VPDs (Variable Phase Delay filters). A frequency selective algorithm is to select the fundamental frequencies in each section. Then either the coherent or incoherent methods has to be implemented to estimate the DOAs.

6.1 Variable Phase Delay filters (VPDs)

Before testing the algorithm whether works or not, an array output for the wideband signal have to be created. In the ULA, the signal received at very left microphone is considered as the reference signal. Then the signal received at the N^{th} microphone is a delay version of the reference one.

$$\tau_i = \frac{(i-1)d\sin(\theta)}{v},\ i = 1, 2, \ldots, N \tag{6.1}$$

In UCA, the reference is taken at the origin of the array. The delay at N^{th} microphone is depending on both the elevation and azimuth angle:

$$\tau_i = \frac{r}{v}\sin(\theta)\cos(\phi - \frac{i-1}{N}),\ i = 1, 2, \ldots, N \tag{6.2}$$

The delay number is defined as the product between the delay time and the sampling frequency. If the delay number is integer, the delayed signal could be achieved by shifting the memory buffer. However, the result is not integer in the most case. Then the variable phase delay filters (VPDs) comes up to solve the problem when delay number is fractional [22].

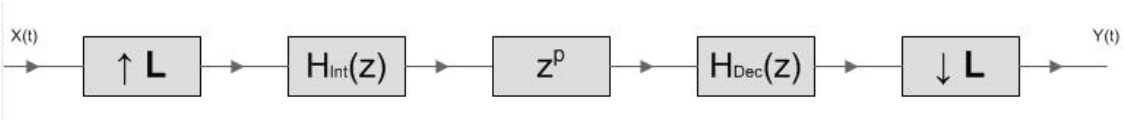

Figure 6.1: Variable Phase Delay filters

Figure 6.1 shows the structure of the VPDs. The VPDs consists of following steps:

- interpolation the signal by L
- get rid of the image signals by using an anti-imaging filter
- delay the signal at high sampling frequency
- pass to an anti-aliasing filter before doing decimation
- decimate the signal by L and back to the original sampling frequency

The L and P are respectively the numerator and denominator of the delay number. In ***Matlab*** the interpolation and anti-imaging filter could be done by calling the function ***interp***, and the decimation including the anti-aliasing filter is done by calling the function ***decimate***.

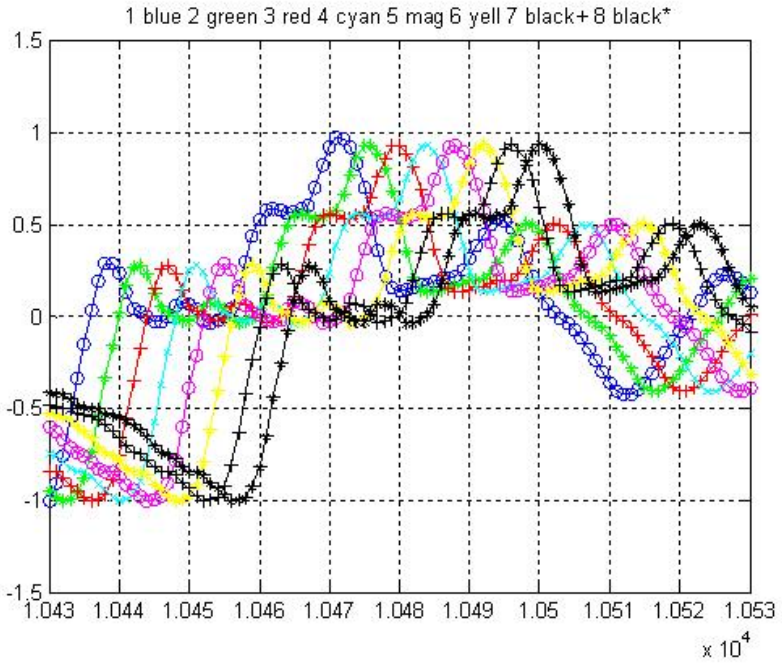

Figure 6.2: Artificial Array Output via VPDs in ULA

Figure 6.2 shows the artificial signals that contain the signal outputs from each microphone in an ULA when the signal locates at 45°. In the ULA, the distance between adjacent microphone is identical. This leads the delay between the adjacent microphone is the same as well.

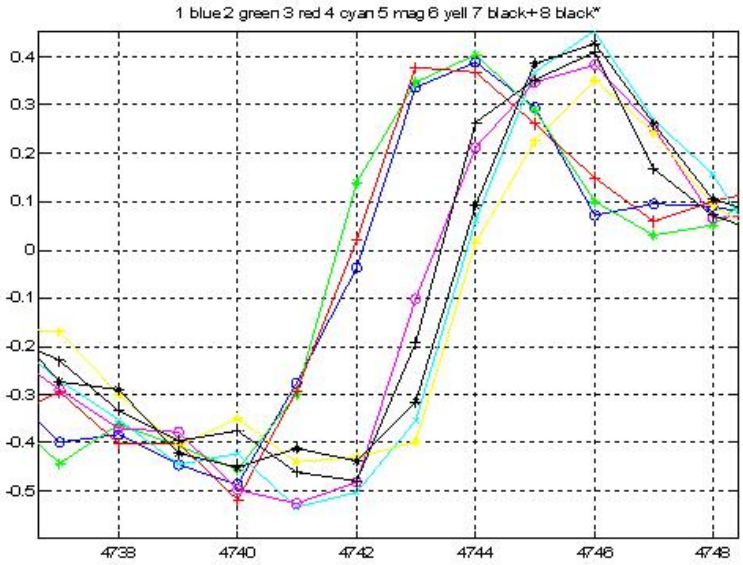

Figure 6.3: Artificial Array Output via VPDs in UCA

Figure 6.3 shows a part of the array output when the elevation signal is equal to 90° and the azimuth angle is equal to 45°. The signal is corrupted by the noise. The signal to noise ratio is equal to 10dB. When the azimuth signal is equal to 45°, the signal received at 2^{nd} microphone leads and the 7^{th} microphone lags. The other pairs of signal (No.1 and No.3, No.4 and No.8, No.5 and No.7) have little phase difference. This is approximately to prove that the artificial signals that created by the VPDs method is correct.

In the later section, VPDs is used to create the artificial signals that are assumed to be the ideal microphone array output (in both ULA and UCA). The created signals is used to test whether the wideband DOA algorithm works.

6.2 Frequency selection

In the narrowband DOA algorithms, the signal consists of only one frequency component. But for normal speech signal, the spectrum locates from 100Hz to 3500Hz, which is not narrowband anymore. Then to analyze the signal spectrum and to get the fundamental frequencies will be very necessary. In the most case, the Fast Fourier Transform (FFT) is used to calculate the spectrum of signal. To reduce the spectrum leakage, a window has to be applied.

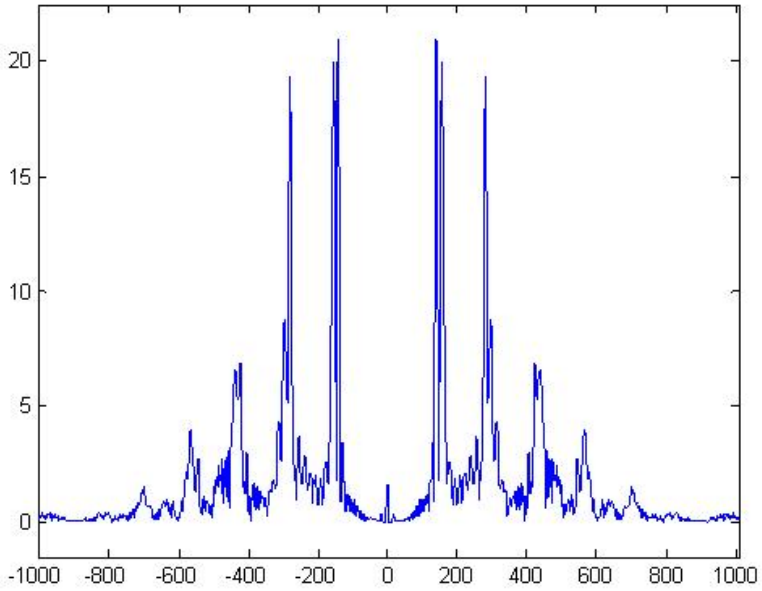

Figure 6.4: Speech signal in frequency domain

In Figure 6.4, it shows the spectrum of the sampled speech signal. It could be noticed that only some of the frequency components do the main contribution. Selecting the frequency components that contain the higher values makes more sense to choose the ones with lower values. The noise is assumed to be white when the signal transmits through the air. Then if the frequency components with high values are selected, the corresponding signal-to-noise ratio at the selected frequency is high as well. Therefore, to calculate the DOA on these frequency components will be more reliable.

The approach in this thesis for selecting the fundamental frequency is to split the whole frequency range into different sections and pick the frequency component with the highest absolute value in each section. All the selected frequencies should be sorted descendingly and the components with the higher values are taken into DOA calculation.

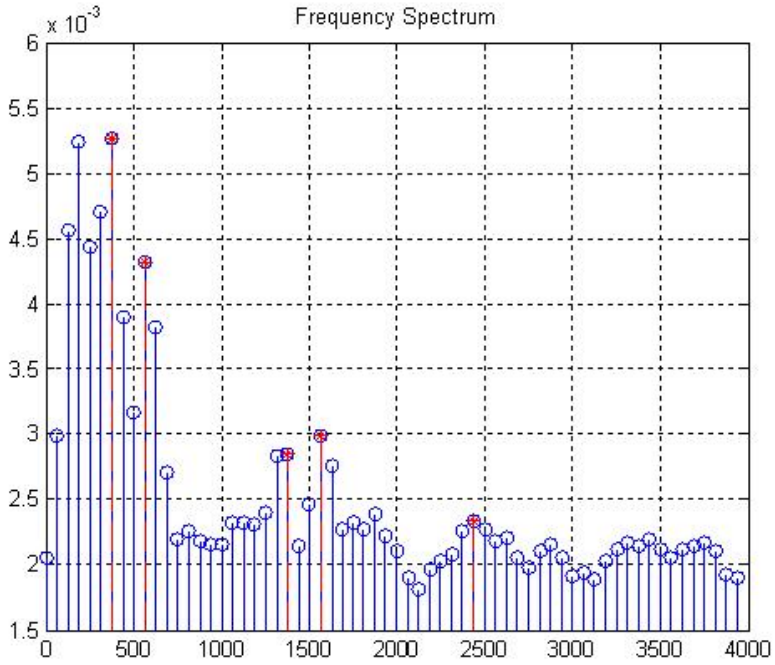

Figure 6.5: Fundamental frequency selection

In Figure 6.5, the frequency components with red color are the fundamental frequency components which are selected via frequency selection algorithm.

6.3 Incoherent wideband DOA algorithms

Now each selected frequency component could be used for narrowband DOA algorithms individually. If the MUSIC algorithm is chosen as the detection algorithm, the final result is just to sum up the MUSIC spectrum and search the peaks, which is the same as the one for narrowband detecting. For the ESPRIT algorithm, the result is achieved by summing up DOAs on each selected frequency and takes the average value. This kind of approaches that calculate the DOAs individually on each frequency is called incoherent method.

6.3.1 Incoherent MUSIC in ULA

When the MUSIC algorithm is applied, different MUSIC spectrums are obtained at different fundamental frequency. After summing up all these MUSIC spectrums, an synthetical MUSIC spectrum is formed.

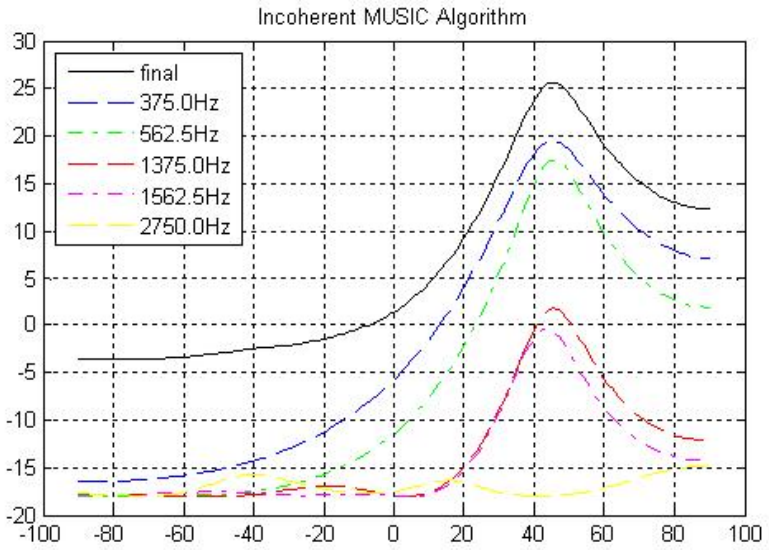

Figure 6.6: Incoherent MUSIC in ULA

Figure 6.6 shows the MUSIC spectrum at each selected frequency when DOA= 45°. Though the spectrum in yellow color tells the wrong DOA information, the final

MUSIC spectrum (in black color) still gives the DOA which is very close to the real one.

6.3.2 Incoherent ESPRIT in ULA

Since the ESPRIT is a close-form DOA algorithm, it will give the estimated DOAs directly instead of a spectrum like MUSIC algorithm. The final DOA could be calculated by averaging the DOAs that are computed at each fundamental frequency.

Incoherent ESPRIT Algorithm with $\theta = 45°$					
Fundamental Frequency (Hz)	375	562.5	1375	1562.5	2437.5
Direction of Arrival θ_i	43.4323°	47.1488°	47.0296°	41.7513°	3.4052°
$\theta = 35.1914°$					

Table 6.1: Incoherent ESPRIT in ULA

Table 6.1 shows the result via the incoherent ESPRIT method. The 3^{rd} row shows the calculating result using narrowband ESPRIT algorithm on each selected frequency. It is apparently to be seen that not all the results are close to the real direction-of-arrival angle. Since the final DOA is obtained by averaging the DOAs calculated on these frequencies. One detection error would cause the imprecision of the final result.

6.3.3 Comparison between incoherent methods in ULA

For the incoherent method in ULA, the result by applying MUSIC algorithm is much better than using the ESPRIT algorithm. The MUSIC algorithm is to calculate the MUSIC spectrum on the selected frequencies and sum up. In the end, the DOA could be achieved by the peak search on the composed MUSIC spectrum.

The ESPRIT is not like MUSIC algorithm. Since it is a closed-form DOA algorithm, it will give the DOAs directly. In case that the DOA that calculated by ESPRIT algorithm at one of the selected frequencies is wrong. The correctness of the

final DOA will be dramatically degraded, because it is calculated by averaging all the DOAs calculated from all selected frequency. The conclusion for incoherent method is that the MUSIC algorithm performs better than the ESPRIT algorithm.

6.3.4 Incoherent UCA-RB-MUSIC

Similar as the MUSIC algorithm in ULA, the UCA-RB-MUSIC is to calculate the spectrum at first as well. The UCA-RB-MUSIC needs a 2-D search algorithm to find the peaks. One dimension is corresponding to the elevation angle, and the other is to the azimuth angle.

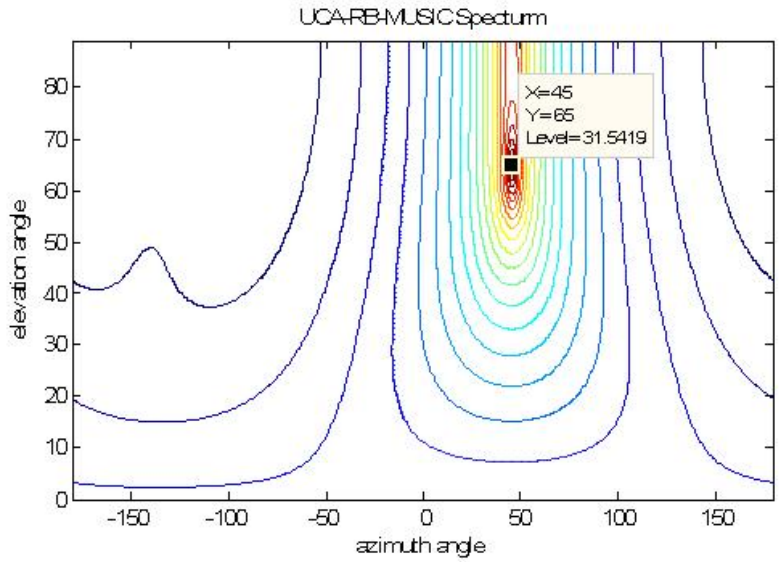

Figure 6.7: Incoherent UCA-RB-MUSIC in UCA

Figure 6.7 shows the contour plot of the final UCA-RB-MUSIC spectrum, which is the summation of the spectrums calculated at the fundamental frequencies. The x axis and y axis are respectively the azimuth angle and the elevation. The peak locates at the position where azimuth angle is 45° and elevation angle is 60°. The real azimuth angle is 45° and elevation angle is 90°. This tells that the algorithm could detect the azimuth angle very accurately, but not for the elevation angle.

In UCA-RB-MUSIC, the spectrum has to be calculated for all detectable angle range. In UCA, the azimuth angle is from $-179°$ to $180°$ and the elevation angle is from $0°$ to $89°$. If the angle resolution is one degree, the calculation of the spectrum will be finish after 32400 (360×90) rounds. In the ULA, the detectable azimuth angle range is from $-89°$ to $90°$ and the elevation angle is out of consideration. Therefore, the calculation of spectrum only needs 180 times. The UCA-RB-MUSIC costs much more time than the MUSIC algorithm in ULA to get the spectrum. Because of this reason, the UCA-RB-MUSIC exists only in the theory part. None of the real-time implementations is using UCA-RB-MUSIC to calculate the DOAs.

6.3.5 Incoherent UCA-ESPRIT

Like the ESPRIT algorithm used for ULA, the UCA-ESPRIT is also a close-form DOA detection algorithm, specially developed for the UCA. In the incoherent ESPRIT, the azimuth angles are firstly calculated at each selected frequency and the mean value of these angles will be the final DOA. It is the almost same for the incoherent UCA-ESPRIT. Only the UCA-ESPRIT needs to average both the azimuth and elevation angles.

Incoherent UCA-ESPRIT Algorithm with $\phi = 45°$, $\theta = 90°$					
Fundamental Frequency (Hz)	375	500	1250	1500	2500
elevation angle θ_i	$90°$	$64.78°$	$68.47°$	$63.37°$	$14.87°$
azimuth angle ϕ_i	$45.25°$	$45.55°$	$46.31°$	$43.29°$	$-145.52°$
$\phi = 6.98°$, $\theta = 60.30°$					

Table 6.2: Incoherent UCA-ESPRIT in UCA

Table 6.2 shows the results when the incoherent UCA-ESPRIT algorithm is applied to calculate the DOA when the signal comes from the direction that $\phi = 45°$ and $\theta = 90°$. The result is strongly corrupted by the DOA calculate at the last frequency.

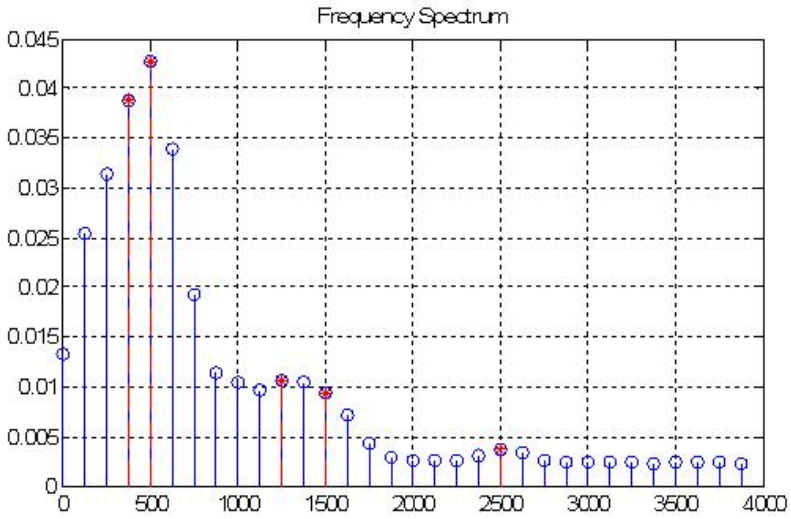

Figure 6.8: frequency spectrum for the signal received at UCA

Figure 6.8 shows the value at frequency 2500Hz is quite small, which implies the SNR is quite low. Then signal at this frequency is strong distorted by the noise, which leads to a very bad DOA estimation. If the last estimation is taken out of the calculation, the final result becomes:

$$\phi = 71.66°, \theta = 45.10°$$

The result was optimized and the azimuth angle at the moment is very close to the real value.

6.3.6 Conclusion of the incoherent method

Incoherent method is to calculate the DOA individually at each selected frequency. Both MUSIC and ESPRIT algorithm could be applied for ULA and UCA. The MUSIC algorithm gives a better result compare to the ESPRIT. If the detection error happens in one of the selected frequencies, the accuracy of detection in ESPRIT algorithm will degrade.

6.4 Coherent Wideband DOA Algorithms

The simulation for incoherent methods has been shown in the last section. Incoherent method needs to calculate the narrowband DOA algorithms several times to get either the spectrum or the DOA at each selected frequency, which depends on which algorithm is used. The MUSIC algorithm needs to calculate the spectrum for all detectable angle range, which is very time consuming but give a better result. The ESPRIT is a close-form algorithm that give the DOA directly, but one wrong result at one frequency will reduce the correctness of the final DOA estimation. Therefore, the coherent method comes out which could reduce the computation complexity and the result is obtain by only applying the narrowband method one time.

6.4.1 coherent signal subspace method (CSSM)

In last chapter, the concept of the coherent signal subspace method (CSSM) is introduced. The core of the algorithm is to form the focusing matrices that transform the steering vector from one frequency to the reference frequency. After focusing all the steering vector, one covariance matrix at the reference frequency could be formed by simply summing up the transformed covariance matrix. Then the narrowband algorithm could be used to calculate the DOA by the covariance matrix at reference frequency.

CSSM using MUSIC Algorithm in ULA

In ULA, the steering vector is a vector that contains the phase difference between signal received at the N^{th} microphone to the reference one.

$$a(\theta) = [1, e^{-j2\pi f d \sin(\theta)/v}, \ldots, e^{-j2\pi f (N-1) d \sin(\theta)/v}]$$

The value of steering vector depends on both the frequency and angle. Assuming the angle is initialized, then the vector is only depending on the frequency. Let define the following parameters:

- $\theta_0 = 45°$, initialized DOA estimation
- $f_r = 1000$Hz, reference frequency
- $f_i = 500$Hz, signal frequency

The focusing matrix Ti is calculated by the following formulas:

$$T_i = V_i U_i^H$$

U_i and V_i are respectively the right and left singular matrices of

$$A(f_r, \theta_f) A^H(f_i, \theta_f)$$

And the calculated focusing matrix should be solve the following minimization problem:

$$\min_{T_i} \|A(f_r, \theta_r) - T_i A(f_i, \theta_r)\|$$

Initialized angle: $\theta_0 = 45°$		
$A(f_i, \theta_r)$	$A(f_r, \theta_r)$	$T_i A(f_i, \theta_r)$
1.0000	1.0000	1.0000
$0.9578 - 0.2873i$	$0.8349 - 0.5504i$	$0.8349 - 0.5504i$
$0.8349 - 0.5504i$	$0.3940 - 0.9191i$	$0.3940 - 0.9191i$
$0.6415 - 0.7671i$	$-0.1769 - 0.9842i$	$-0.1769 - 0.9842i$
$0.3940 - 0.9191i$	$-0.6895 - 0.7243i$	$-0.6895 - 0.7243i$
$0.1133 - 0.9936i$	$-0.9743 - 0.2252i$	$-0.9743 - 0.2252i$
$-0.1769 - 0.9842i$	$-0.9374 + 0.3483i$	$-0.9374 + 0.3483i$
$-0.4523 - 0.8919i$	$-0.5909 + 0.8067i$	$-0.5909 + 0.8067i$

Table 6.3: Focusing matrix for MUSIC in ULA

Table 6.3 proves that the focusing matrix T_i realizes the minimization problem above. In fact, the steering vector after focusing is the exactly the same as the one at the reference frequency. Then the focusing matrix for the other frequencies could be obtained by repeating the same steps. Then the covariance matrices after focusing to the reference frequency need to be summed up to form a synthesized covariance

matrix.

$$R_{com} = \sum_{i=kl}^{ku} \alpha_i T_i R_i T_i^H$$

The synthesized covariance matrix could be applied for the MUSIC algorithm. The DOA angle could be calculated via the same steps in the narrowband MUSIC algorithm.

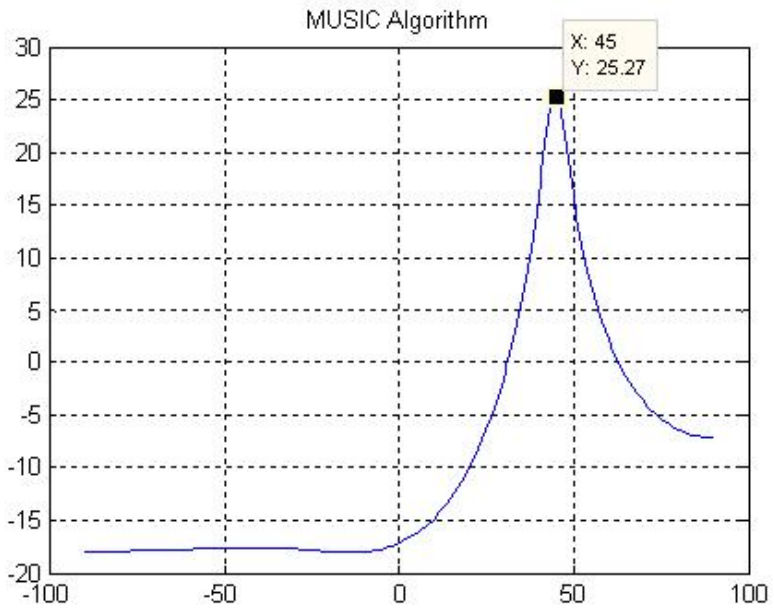

Figure 6.9: coherent MUSIC algorithm with initial angle $\theta_0 = 45°$

Figure 6.9 shows the spectrum that using the coherent method with initial angle 45°. The peak of the spectrum locates exactly at 45°.

But the initial angle normally won't be the same as the real DOA angle. The wrong initial angle will form an imperfective focusing matrix, which leads an imprecision detection result.

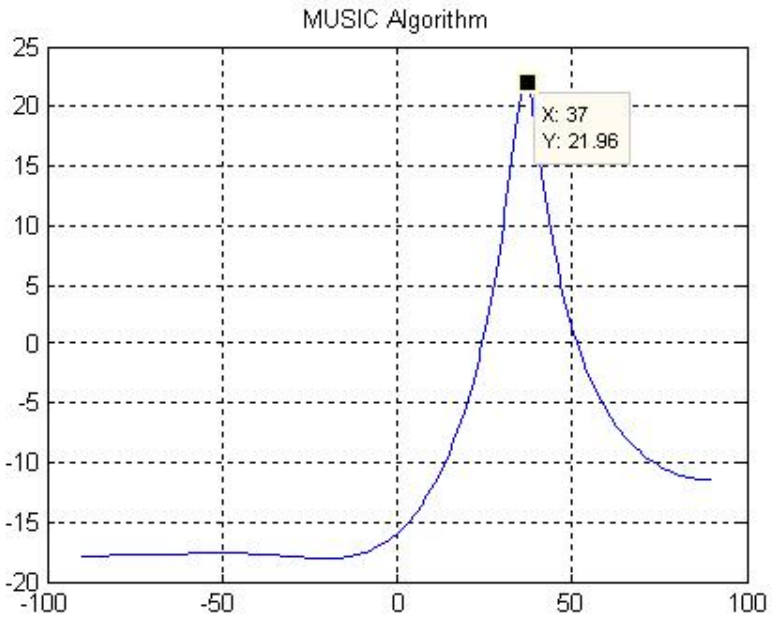

Figure 6.10: coherent MUSIC algorithm with initial angle $\theta_0 = 30°$

Figure 6.10 shows the spectrum when the initial angle is changed to 30°. The peak in this case locates at 37°. This tells the initial angle will decide the accuracy of the detecting result. If the initial angle is not close to the real DOA, the detection result by the coherent method is not reliable as well.

CSSM using ESPRIT algorithm in ULA

To form the focusing matrix for ESPRIT algorithm, the focusing matrices for each subarray should be calculated at first. Then these two focusing matrices is combined into one matrix.

θ_0	θ
45°	45.5163°
30°	36.9162°
60°	54.2659°

Table 6.4: Coherent Signal Subspace Method using ESPRIT in ULA

Table 6.4 shows the results calculated by applying the focusing matrix for ESPRIT algorithm. The real DOA is 45°. Only when the initial angle is close to the real DOA, then the result will be correct. Therefore, the initial angle decides the performance of the coherent signal subspace methods, no matter whether MUSIC or ESPRIT algorithm is applied.

Above all, the conclusion is that the focusing matrix could do the job to transform the covariance matrices from one frequency to reference one, if an initial angle is given. This procedure is also call focusing. The initial angle is very importance to form the focusing matrix. If the angle is closer to the real DOA, the detecting result will be more precise and vise versa.

Then instead that the focusing matrix is formed by single given angle, an angle region around the focusing angle is used. This will compensate the problem when the initial angle with slight bias. Applying the CSM method recursively could achieve better result.

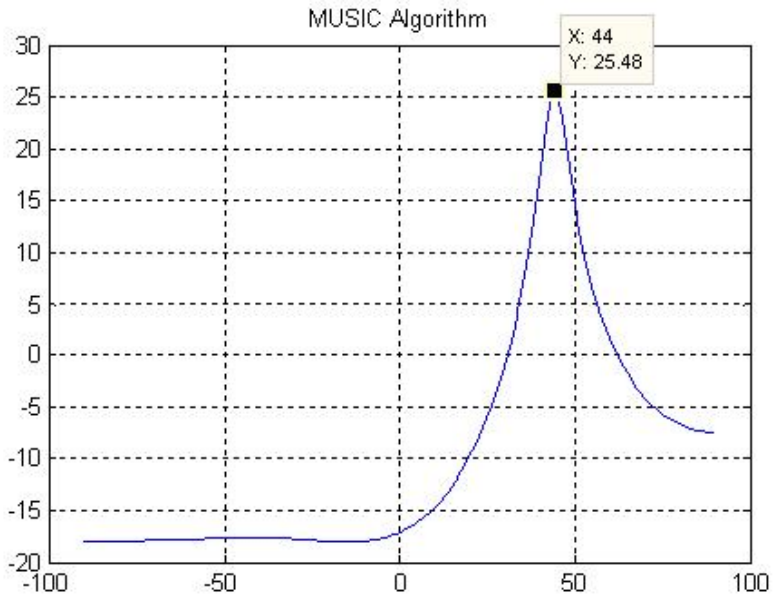

Figure 6.11: recursive CSM using MUSIC in ULA

Figure 6.11 shows the the recursive coherent signal subspace method using MUSIC

algorithm. The initial angle is 30°. The focusing range is from 10° to 50° at first. After repeat the CSM three times, the peaks locates at 44°, which is very close to the real DOA.

Initialized angle: $\theta_0 = 30°$				
1^{st}	2^{nd}	3^{rd}	4^{th}	5^{th}
36.9162°	40.0349°	44.0180°	45.0760°	45.0572°

Table 6.5: recursive CSM using ESPRIT in ULA

It is also the same for doing recursive coherent signal subspace method using ESPRIT algorithm. Table 6.5 shows the results when the initial angle is 30°. After each calculation, the resulting DOA angle is closer to the real DOA. In the end, a very accurate result is obtained.

6.4.2 Robust Coherent Signal Subspace Method

The recursive CSM algorithm allows only certain amount bias for the initial angle. When the angle is out of this range, the DOA detection will fail again. Therefore, robust coherent signal subspace method (R-CSM) is developed. The big difference between normal CSM method and R-CSM is that no initial angle is needed for R-CSM. In ULA, the detectable angle range is from $-89°$ to 90°. Similar as the recursive CSM that the focusing matrix is developed based on a given angle range, the difference is that for R-CSM the very first focusing matrix is formed upon all the detectable angle range. Applying this focusing matrix to get the synthesized covariance matrix at reference frequency, the initial angle could be computed by either MUSIC or ESPRIT algorithm. And afterwards, reduce the focusing range around focusing angle and repeat the CSM methods until the result is getting stable.

R-CSM using MUSIC algorithm in ULA

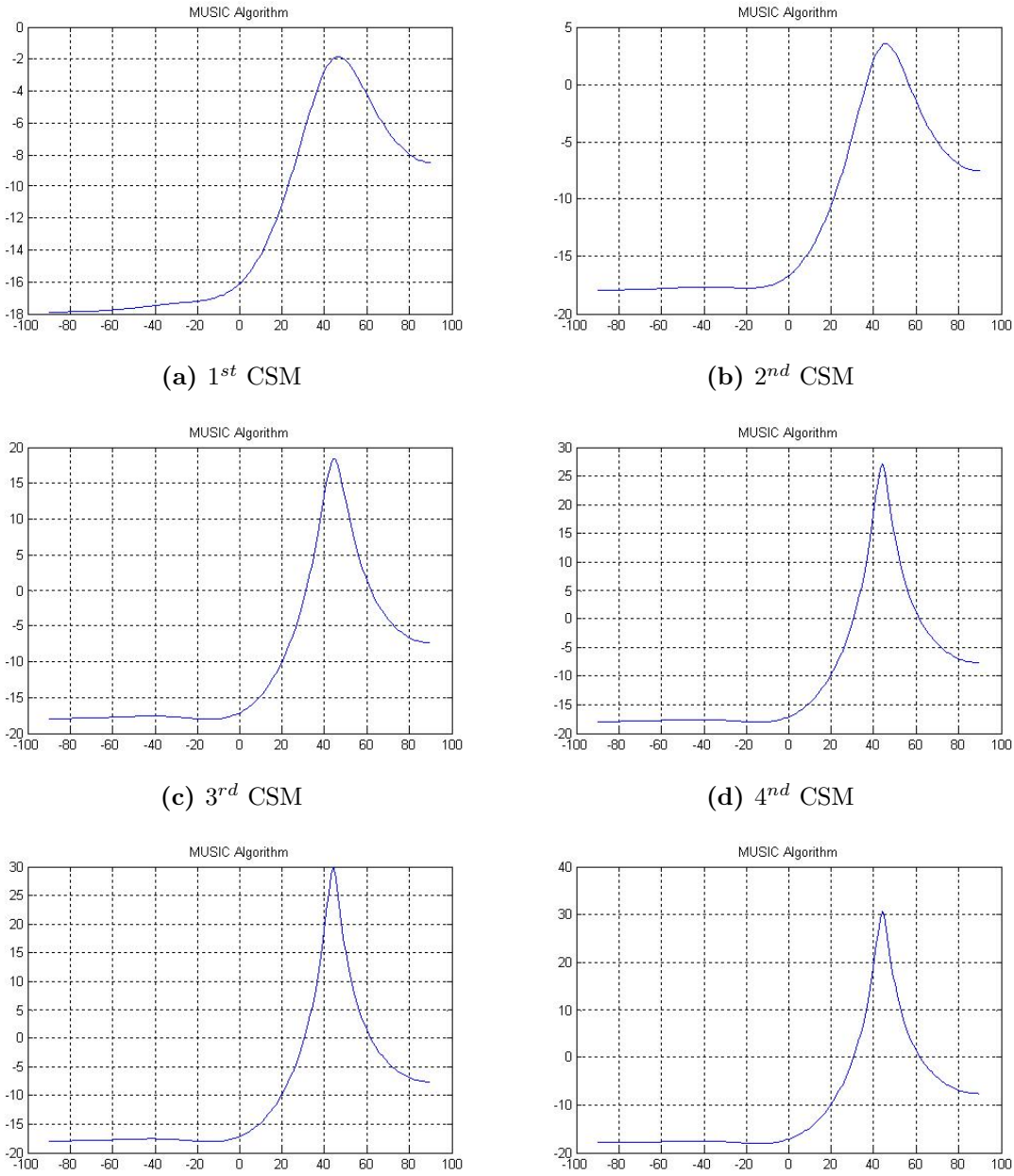

(a) 1^{st} CSM **(b)** 2^{nd} CSM

(c) 3^{rd} CSM **(d)** 4^{nd} CSM

(e) 5^{rd} CSM **(f)** 6^{nd} CSM

Figure 6.12: Robust-CSM using MUSIC algorithm

Figure 6.12 shows the spectrum after each round. The 1^{st} detection result gives a spectrum with a flat peak, meanwhile the focusing angle is obtained. By repeating the calculation, the peak is getting sharper and the value of the peak is getting higher as well. In the end, the peak locates at the expected angle.

R-CSM using ESPRIT algorithm in ULA

Robust-CSM can also applied for the ESPRIT algorithm.

1^{st}	2^{nd}	3^{rd}	4^{th}	5^{th}	6^{th}
42.1524°	42.9878°	43.5482°	43.8602°	43.9290°	43.9578°

Table 6.6: robust-CSM using ESPRIT

The real DOA is 45°. In table 6.6, it shows the 1^{st} calculation DOA angle is already very close to the real one. After certain amount of the iterative calculation, the result gets closer to the real DOA angle.

The majority advantage of using R-CSM compare to normal CSSM is that it doesn't any initial angle. The initial angle could be obtained after 1^{st} iteration. The normal CSSM is faster than R-CSM, but need an initial angle which is close to the real DOA, otherwise the detection could be failed.

6.4.3 Coherent Signal Subspace Method in UCA

In the UCA, the focusing matrix is developed in different way. In the last chapter, the formula how to develop the focusing matrix is introduced. The steering matrix need to be transform from element space to beamspace first. After focusing the beamspace steering vector, the transformed beamspace steering vector at reference frequency needs to be transform back to the element space. To successfully applied the CSSM in UCA, the elevation should be equal to 90°, which means that the speech signal comes

from quite far away.
The element-space steering vector in UCA is:

$$\varphi_m = kr \sin\theta \cos(\phi - 2\pi \frac{n-1}{N}), \text{ where } k = \frac{2\pi}{\lambda}$$

After applying the phase mode excitation, the element-space steering vector is transformed into beamspace:

$$f_m^c(\theta) = \frac{1}{N} \sum_{n=0}^{N-1} e^{jm\gamma_n} e^{j\zeta cos(\phi - \gamma_n)} = j^m J_m(\zeta) e^{jm\phi}$$

To prove that the focusing matrix works fine for both element-space and beamspace, some initializations are made as followings:

- $\phi = 120°$, azimuth angle
- $\theta = 90°$, elevation angle
- $fj = 500$, signal frequency need to be focused
- $fr = 1000$, reference frequency
- $N = 8$, number of microphone
- $M = 3$, maximum phase mode

The focusing matrix is formed via the equation:

$$T_i = F^{-1} B_m F$$

where $B_m = J_m(\zeta_0)/J_m(\zeta)$

$A(f_i)$	$A(f_r)$	$T_iA(f_i)$
$0.9788 - 0.2046i$	$0.9163 - 0.4006i$	$0.9174 - 0.4005i$
$0.9943 + 0.1065i$	$0.9773 + 0.2117i$	$0.9762 + 0.2116i$
$0.9370 + 0.3494i$	$0.7558 + 0.6548i$	$0.7570 + 0.6549i$
$0.9218 + 0.3877i$	$0.6994 + 0.7147i$	$0.6982 + 0.7147i$
$0.9788 + 0.2046i$	$0.9163 + 0.4006i$	$0.9174 + 0.4005i$
$0.9943 - 0.1065i$	$0.9773 - 0.2117i$	$0.9762 - 0.2116i$
$0.9370 - 0.3494i$	$0.7558 - 0.6548i$	$0.7570 - 0.6549i$
$0.9218 - 0.3877i$	$0.6994 - 0.7147i$	$0.6982 - 0.7147i$

Table 6.7: Focusing matrix for UCA

Table 6.7 shows the steering vector before focusing after focusing. The steering vector after focusing is very close to the one before focusing. Therefore, the focusing matrix could transform the steering vector from 500Hz to 1000Hz with slight change.

$$T_iA(f_i) - A(f_r) = \begin{bmatrix} -0.0012 - 0.0001i \\ 0.0012 + 0.0001i \\ -0.0011 - 0.0001i \\ 0.0012 + 0.0000i \\ -0.0012 + 0.0001i \\ 0.0012 - 0.0001i \\ -0.0011 + 0.0001i \\ 0.0012 - 0.0000i \end{bmatrix}$$

This bias is caused by transformation between element space and beamspace. The inverse of the beamformer multiplying itself doesn't give an identity matrix. The error varies when the reference frequency or the azimuth angle changes. Compare to the steering vector at the reference frequency, the error is quite small. Therefore, these bias could be ignored. Then the focusing matrices for all the frequency need to be calculated and focusing all the covariance matrices to the reference frequency. The narrowband DOA algorithm, (UCA-RB-MUSIC or UCA-ESPRIT) could be applied.

To prove the correctness of the focusing matrix, an artificial array output is created by the VPDs. Then the results before and after focusing are compared. The algorithm applied here is UCA-ESPRIT.

$N = 16$, $\theta = 90\circ$, $\phi = 45\circ$ $f = 500$, $f_r = 1000$	No noise	SNR = 5dB	SNR = 20dB
Before focusing	$\theta = 88.97°$ $\phi = 45.00°$	$\theta = 72.28°$ $\phi = 46.41°$	$\theta = 90.00°$ $\phi = 45.01°$
After focusing	$\theta = 90.00°$ $\phi = 45.00°$	$\theta = 88.97°$ $\phi = 45.00°$	$\theta = 90.00°$ $\phi = 45.76°$
Difference	$\theta = 1.03°$ $\phi = 0.00°$	$\theta = 16.69°$ $\phi = -1.41°$	$\theta = 0.00°$ $\phi = 0.77°$

Table 6.8: focusing matrix testing for narrowband signal

Table 6.8 shows the deviation between the result calculated directly using UCA-ESPRIT and the one after applying focusing matrix. Here the number of microphone is 16. The elevation angle is fixed to 90° and the azimuth angle is set to 45°. The results tells the difference between the one before focusing and the one after focusing won't be much when the SNR is high. In the case that SNR is low, the detection result for azimuth angle is still very promising. Then it could be concluded that focusing matrix does the job that transforms the signal from one frequency to the other.

To successful detect the DOA for the wideband signal, a set of focusing matrices has to be formed that could transform the signal components at all frequencies to one reference frequency. Then either the UCA-RB-MUSIC algorithm is applied to calculate the 2-D MUSIC spectrum or The UCA-ESPRIT algorithm is used to calculate the DOA directly.

UCA-RB-MUSIC with CSSM

After calculating the focusing matrix for all the frequency bins. The coherent covariance matrix reference frequency could be formed via:

$$R_{com} = \sum_{i=kl}^{ku} \alpha_i T_i R_i T_i^H \tag{6.3}$$

The approach is the same as what has been explained for the coherent wideband DOA detection in ULA. Then UCA-RB-MUSIC could be applied to calculate the 2-D MUSIC spectrum at the reference frequency. The corresponding azimuth and elevation where the peak locates will be the expected DOA.

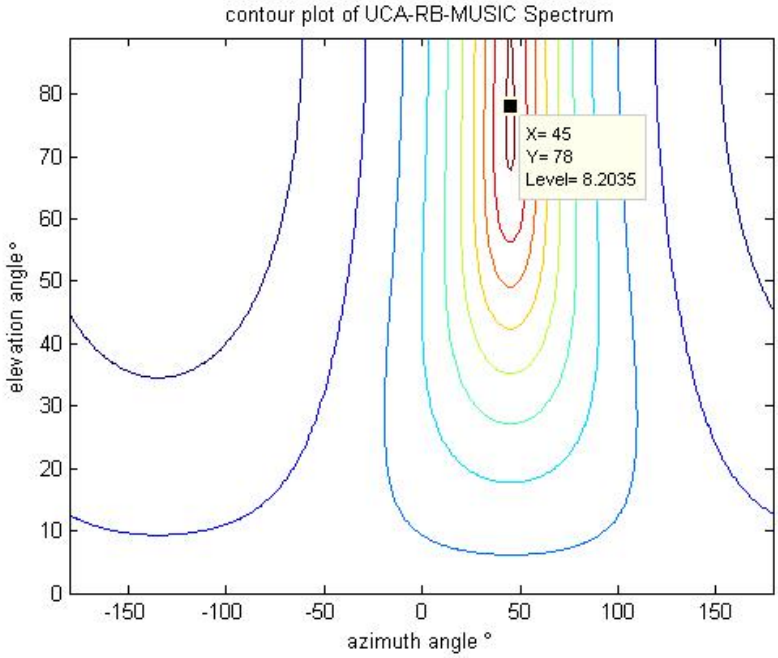

Figure 6.13: contour plot for coherent UCA-RB-MUSIC

Figure 6.13 shows the contour plot of the UCA-RB-MUSIC spectrum when the signal source locates at $\theta = 90°$ and $\phi = 45°$. The signal-to-noise ratio is equal to 20dB. The peak of the calculated spectrum locates at the position where $\theta = 78°$ and $\phi = 45°$, which gives a correct azimuthal detection result. The result of the elevation angle is imprecise. Here, the array consists of 16 microphones. The number of microphone is not big enough to give a precise detection result for the elevation angle. More tests will be proceeded in the UCA-ESPRIT.

UCA-ESPRIT with CSSM

As introduced before, the UCA-RB-MUSIC is not suitable to be applied for the hardware implementation. The UCA-RB-MUSIC needs to calculate the spectrum at all

possible angle range. In addition, a 2D peak search has to be developed to find the position of the peaks. Both of them cause the slowness of the algorithm. Therefore, using the close-form algorithm UCA-ESPRIT is preferable. Normally the performance of the algorithm is depending on the following parameters:

- azimuth angle(θ)
- elevation angles (ϕ)
- signal-to-noise ratio (SNR)
- number of the microphone (N)

Since the coherent signal subspace method is developed in the case that elevation is equal to 90°, therefore the elevation angle is keeping fixed and equal to 90°.

SNR = 20dB,$\phi = 45\circ$	$N = 8$	$N = 16$	$N = 32$
calculated result	$\theta = 66.35°$ $\phi = 44.48°$	$\theta = 71.47°$ $\phi = 44.47°$	$\theta = 78.41°$ $\phi = 45.06°$
deviation	$\theta = -23.65°$ $\phi = -0.52°$	$\theta = -18.53°$ $\phi = -0.5254°$	$\theta = -11.58°$ $\phi = 0.06°$

Table 6.9: coherent wideband UCA-ESPRIT 1

Table 6.9 shows the simulation results using UCA-ESPRIT with different number of microphones. The deviation shows the difference between the calculated result and expected angle. With the increment of the number of microphone, the elevation angle is getting closer to the expected value. The azimuth angle doesn't change much when the number of microphone increases.

N = 16,$\phi = 45\circ$	SNR = 5dB	SNR = 20dB	no noise
calculated result	$\theta = 90.00°$ $\phi = 44.02°$	$\theta = 71.47°$ $\phi = 44.47°$	$\theta = 72.78°$ $\phi = 45.00°$
deviation	$\theta = 0.00°$ $\phi = -0.98°$	$\theta = -18.53°$ $\phi = -0.5254°$	$\theta = -17.22°$ $\phi = 0.00°$

Table 6.10: coherent wideband UCA-ESPRIT 2

Table 6.10 shows the simulation results using UCA-ESPRIT with different signal-to-noise ratio. The signal source locates at the fixed direction. The number of microphone is set to 16. When the noise is white sense, the detection result for the azimuth angle is still promising even in the case that SNR is low. The accuracy of the elevation result is not good.

N = 16, SNR = 20dB	$\phi = -60°$	$\phi = 45°$	$\phi = 120°$	$\phi = -140°$
calculated result	$\theta = 77.24°$ $\phi = -58.71°$	$\theta = 71.47°$ $\phi = 44.47°$	$\theta = 79.33°$ $\phi = 120.12°$	$\theta = 82.36°$ $\phi = -140.11°$
deviation	$\theta = -12.76°$ $\phi = 1.29°$	$\theta = -18.53°$ $\phi = -0.5254°$	$\theta = -10.67°$ $\phi = 0.12°$	$\theta = -7.64°$ $\phi = -0.11°$

Table 6.11: coherent wideband UCA-ESPRIT 3

Table 6.11 shows the results when the source locates at different directions. The result of the azimuth angle is of little deviation. These azimuth angles are taken from each quadrant, which proves that the algorithm could detect the 360° azimuthal angle. The elevation angle is comparable not as precise as the azimuth.

Above all, the tests have been made to check the performance of the coherent wideband UCA-ESPRIT algorithm by varying the number of microphones, signal-to-noise ratio and azimuth angle. The results shows the accurate azimuthal detection requires not much hardware demanding. On the contrary, the accuracy of the elevation angle detection is not good even when a high number of microphone is applied.

For the project, the main goal is detecting the azimuthal angle correctly. The elevation angle detection is an alternative. Therefore, the imprecision of the elevation detecting result could be neglectable. In the next chapter, the real-time system will be implemented which is based on this coherent wideband UCA-ESPRIT algorithm.

Chapter 7

Real-time Implementation

In the previous chapter, the simulation has been presented for calculating DOA when the signal is wideband. The coherent method gives a faster calculation if the ESPRIT algorithm is chosen. The final goal of the project is to design a system that could detect 360° azimuth angle range. Therefore, the UCA-ESPRIT will be chosen to be implemented for the real-time system.

This chapter consists of the following parts. At first, the hardware settings are going to be introduced. Then the steps for the implementation will be explained. In the end, the test results will be analyzed and the performance of the system will be discussed.

7.1 Hardware Settings

7.1.1 DSK6713 + PCM3003

The board used for the real-time implementation is DSK6713 with the daughter board PCM3003. The PCM3003 is an eight channel 16-bit audio codec daughter board, suitable for the D.Module Family of DSP Computer Modules. The eight A/D and D/A converters are sampled synchronously. The PCM3003 Delta-Sigma converters provide excellent dynamic characteristics and inherent anti-aliasing and reconstruction filtering.

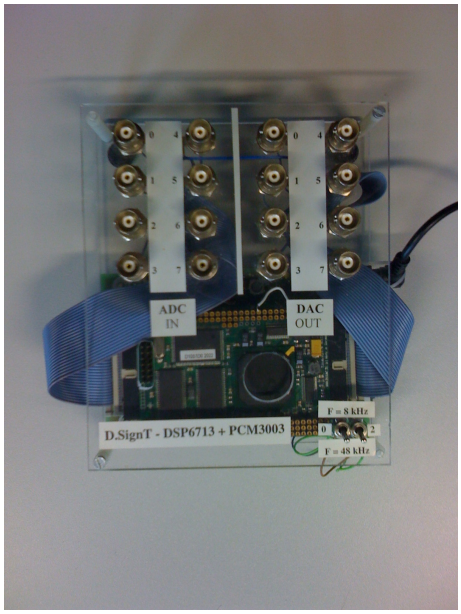

Figure 7.1: DSK6713 + PCM3003

Figure 7.1 shows the TI-board DSK6713 with the daughter board PCM3003. More details about the board could be found in the Master thesis of Mr. Saxena [6].

7.1.2 Uniform Circular Array

To implement UCA-ESPRIT algorithm, a uniform circular array is made which contains eight microphones. Each microphone is connected with a pre-amplifier. The

diameter of the microphone array is 9cm. The distance between the adjacent microphones is then approximately equal to 3.44cm. To avoid spatial aliasing, the maximum frequency has to be less than 5000Hz. Since the speech signal only locates from frequency 100Hz to 3500Hz. The distance fulfills the requirement. Figure 7.2 shows the setup of the Uniform Circular Array.

Figure 7.2: Uniform Circular Array (UCA)

7.2 Implementation of the algorithm

In the previous chapter, the basic concept of the UCA-ESPRIT has been introduced. To successfully develop the coherent UCA-ESPRIT in real time, the following steps shown in the following flow chart have to be implemented.

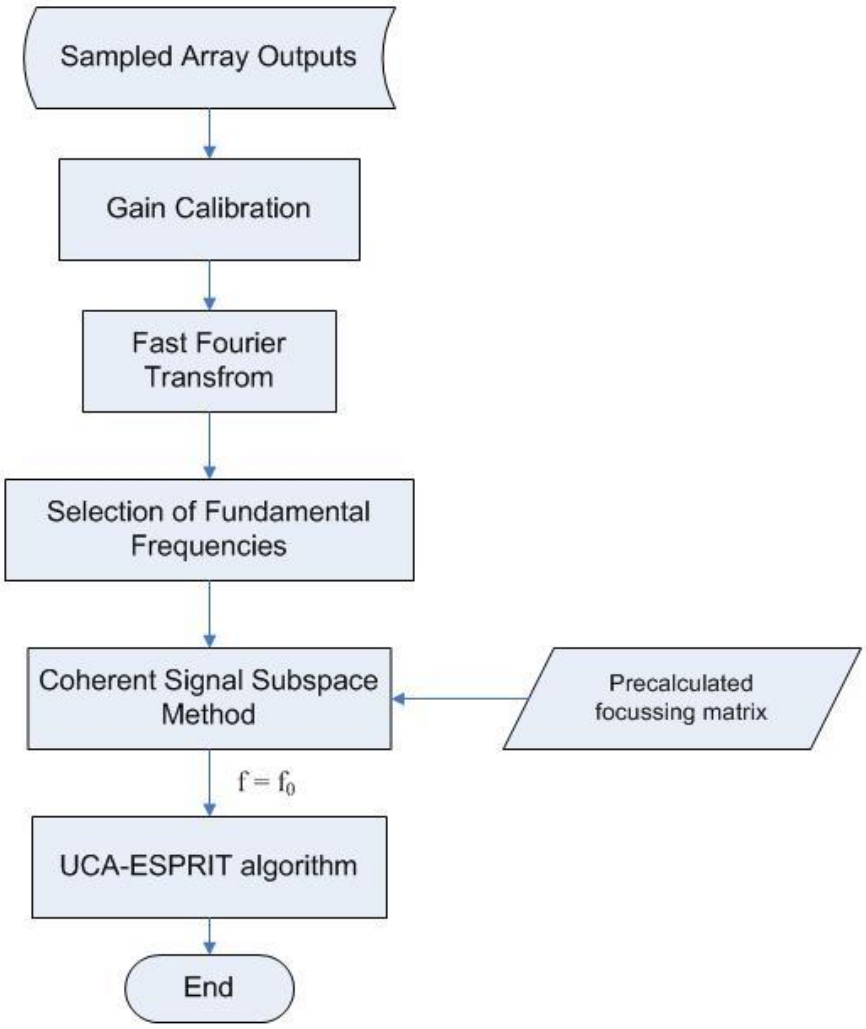

Figure 7.3: real time implement of UCA-ESPRIT algorithm

7.2.1 Ping-Pong Buffering

The Ping-Pong Buffering is to use two buffers to store the sample date continuously to avoid the situation that the data in the buffer changes during the processing. While the EDMA is transferring the data into the Ping buffer, the CPU does the processing in Pong buffer.

The interrupt routine *edma_complete_int(void)* is to check which EDMA buffer is completed. When the flag *block* is equal to 0, it means the Ping buffer is complete. When the flag *block* is equal to 1, it means the Pong buffer is complete. In the program, it is only necessary to check whether a new block is complete. Therefore, the flag *block* is initialized to -1 after each calculation. A while loop is created to wait until the value of the flag changes.

7.2.2 Distinguishing between noise and signal

After the buffer is full, the main program starts. But it doesn't know at first whether the data stored in the buffer is the speech signal or just the noise. There is no sense to proceed the algorithm when only the silence signal was taped. To distinguish the data in the buffer whether is speech or noise, the power of signal was calculated. A threshold is defined in preliminary. When the power exceed the threshold, it is assumed that the input data is speech signal and the algorithm could be proceeded. Otherwise, the program has to wait until the next buffer is full.

7.2.3 Amplitude calibration

In the simulation, the VPDs method creates the artificial signals for the array output. The signals received at microphones are assumed to be identical. However in reality, the microphone normally has difference sensitivity, which causes the different attenuation factors. Therefore the signal arrived at each microphone has to be calibrated in the beginning.

Here a very simple method is developed to realize the gain calibration. The power of the sampled speech signal at each microphone is calculated at first. Then gain ratio is obtained by calculating the square root of the ratio between the powers of N^{th} microphone and the 1^{st} one. When the gain ratio is calculate, the calibrated signal will be obtained by

$$\bar{x_i} = \alpha_i x_i$$

where α_i is the gain ratio between the N^{th} microphone and the 1^{st} one.

7.2.4 Fast Fourier Transform

Before selecting the fundamental frequencies, the spectrum of the input signal has to be calculated. The FFT algorithm used in the program is from TMS320C6713 DSP library [17]. It consists of following functions:

gen_w_r2(W, BUFLEN);
bit_rev(W, BUFLEN $\ll$ 1);
cfftr2_dit(x_fft, W, BUFLEN);
bit_rev(x_fft, BUFLEN);

To save the calculation load, the twiddle factor W needs to be calculated once before the main program and pass to the function as a parameter.

7.2.5 Adaptive selection of fundamental frequencies

After the complex value spectrum is calculated, the power spectrum could be obtained by simply sum up the square value of the real and imaginary parts. The whole frequency range could be separated into several bins. Then the fundamental frequencies could be obtained by searching the peak values in each bin. Then all the peak values will be sorted descendingly. The corresponding frequencies with the highest peak values will be the selected fundamental frequencies.

7.2.6 Coherent Covariance Matrix

Now the fundamental frequencies have been calculated. The covariance matrices at the selected frequency could be formed.

$$R_i = X_i X_i^H;$$

As introduced in the previous chapter, the focusing matrix is used to translate the steering vector from one frequency to the reference one. Here the focusing matrices for all the frequencies have been pre-calculated. Then the coherent covariance matrix could be calculated via

$$R_{com} = \sum_{i=1}^{K} T_i R_i T_i^H;$$

7.2.7 Element-space to Beam-space

When the coherent covariance is formed, then the classic UCA-ESPRIT could be applied for detecting the DOAs. The first step of UCA-ESPRIT is to transform the covariance from element-space to beamspace by using beamforming matrix. The beamforming matrix is determined by the maximum phase mode (M) and number of microphones (N). Therefore, the beamforming matrix could be pre-calculated to save computation load. In the introduction of the UCA-ESPRIT, it has been shown that the algorithm only needs the real-part of the covariance matrix. Then the function *elementToBeamspace(Rcom, cov_fmatrix)* is made to realized the followings:

$$F_r^H R_{com} F_r;$$

The result will be the beamspace covariance matrix at the reference frequency.

7.2.8 Singular Value Decomposition

After transforming the coherent covariance matrix from element space to beamspace, the matrix has to be applied for a decomposition function to extract the signal subspaces. As introduced in the theory, the UCA-ESPRIT only requires a real-value

decomposition. Unlike the complex value decomposition applied for MUSIC and ESPRIT in ULA, the real-value decomposition makes the real-time system faster.

The method is already implemented by Mrs Bing Li and Mrs Yuan Cheng in their thesis [16]. The function called is

svdcmp(cov_matrix_real,2*M+1,2*M+1,svd_u,svd_v)

After transformation, the beamspace covariance matrix has the dimension $(2\mathbf{M}+1) \times (2\mathbf{M}+1)$, where $\mathbf{M}$ is the maximum phase mode. Therefore, the dimension of the column vector svd_u is equal to the one of the row vector svd_v, which is equal to $(2\mathbf{M}+1)$. And the first row of the column vector is the beamspace signal subspace.

7.2.9 Calculation of the DOAs

Then according to the introduction of the UCA-ESPRIT algorithm, the signal subspace vector needs to be separated into three sub-vectors at first. Afterwards, three block matrices B, C, Q are formed via:

$$B = S_{-1}^{H} S_{-1}$$

$$C = S_{-1}^{H} D \tilde{I} S_{-1}^{*}$$

$$Q = S_{-1}^{H} \Gamma S_{0}$$

The corresponding methods that are created to realized these equations are the followings:

B = B_cal(S_Minus);

C = C_cal(S_Minus,S_Plus);

Q = Q_cal(S_Minus,S_Zero,freq);

The complex value Ψ could be obtained via the function

$$\text{Psi} = \text{Psi\_cal(B,C,Q);}$$

The calculated complex value Ψ contains the information of both the elevation and azimuth angles.

$$\theta = sin^{(-1)}(\sqrt{\Psi_R \Psi_R + \Psi_I \Psi_I})$$

$$\phi = tan^{-1}(\Psi_I / \Psi_M)$$

When the azimuth is calculated, the quadrant could be determined by the sign of the real and image parts of the Ψ. When the magnitude of the Ψ is larger than 1, it is not possible to calculate the *arcsin* value. In this case, the elevation angle is simply assigned to 90°.

7.3 Testing Results

Two real-time systems are set up. One is to detect the narrowband signal, which the signal source is a sinusoidal wave with certain frequency. In the narrowband real-time system, there is no need to select certain amount of fundamental frequencies, because the sinusoidal wave only contains only one frequency component. In addition, in stead of doing classic DOA detect at reference frequency after focusing the covariance matrix, the narrowband real-time system is directly applied for the covariance matrix at the fundamental frequency.

The other real-time system is implemented based on the coherent wideband UCA-ESPRIT algorithm. Here certain number of the frequency components that have the higher magnitudes are selected. The covariance matrices on these frequencies are translated into the reference frequency by using focusing matrix. The narrowband UCA-ESPRIT algorithm then calculate the DOA with the covariance matrix at reference frequency. The normal speech signal or a piece of music sound could be used as the signal source.

7.3.1 Testing Environment

Both the narrowband testing and wideband testing are done in a lab room. The signal is corrupted by the noise such as the PC sound, air-condition, and the reverberation signals. To successfully applied the UCA-ESPRIT algorithm, the noise is assumed to be white. In the reality, it is always not realistic.

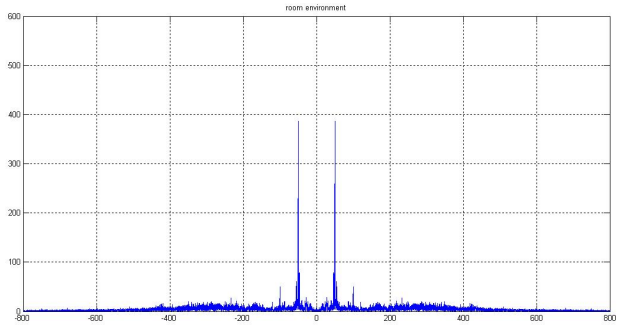

Figure 7.4: Spectrum of the noise in the lab room

Figure 7.4 shows the spectrum of the signal received at 1^{st} microphone when there is no signal source applied. It is obvious to notice that the noise is not white here. There is one 50Hz frequency component which caused by the power supply. The other frequencies components are comparatively very low, which could be neglectable. For the fundamental frequency selection in the algorithm, the frequency will be selected between the range 100Hz and 3500Hz. Therefore, the frequency component below 100Hz won't be taken into consideration. In another word, the 50Hz power line noise won't affect the detecting result.

7.3.2 Testing Results for Narrowband Signals

The sinusoidal signals with different frequencies are applied to test the accuracy of the narrowband real-time system. The test result is shown in the followings.

Freq = 500Hz, Amp = 2V								
Real DOAs (°)	0	45	90	135	180	-45	-90	-135
Testing results (°)	7.5	49.2	91.7	137.5	-179.2	-37.8	-83.6	-129.1
Deviation	7.5	4.2	1.7	2.5	0.8	7.2	6.4	5.9
Average deviation = 4.53°								

Table 7.1: Testing results in real-time system for narrowband signal 1

Freq = 800Hz, Amp = 1V								
Real DOAs (°)	0	45	90	135	180	-45	-90	-135
Testing results (°)	1.8	41.8	86.3	131.5	-187.6	-45.0	-81.7	-135.9
Deviation	1.8	3.2	3.7	3.5	7.6	0	8.3	0.9
Average deviation = 3.63°								

Table 7.2: Testing results in real-time system for narrowband signal 2

Freq = 1500Hz, Amp = 500mV								
Real DOAs (°)	0	45	90	135	180	-45	-90	-135
Testing results (°)	-4.1	39.6	81.2	125.3	-189.5	-51.0	-97.2	-144.2
Deviation	4.1	5.4	8.8	9.7	9.5	6	7.2	9.2
Average deviation = 7.49°								

Table 7.3: Testing results in real-time system for narrowband signal 3

Table 7.1 - 7.3 show the testing results for detecting the sinusoidal signal with $f_1 = 500Hz$, $f_2 = 800Hz$, $f_3 = 500Hz$. The deviations have slight change when the signal frequency changes. The error between the calculate results and real DOA angle is smaller than 10°. This proves the UCA-ESPRIT could localize the speaker with small error. The initial DOA angles are chosen from four quadrants, which covers 360° azimuthal angle. This tells that the UCA-ESPRIT can detect the angle from all azimuthal direction.

7.3.3 Testing Results for Normal Speech

The coherent UCA-ESPRIT algorithm is implemented for localizing the wideband signal source. To test the performance of the real-time application, the speaker speaks from different directions to see the correctness of the result.

Real DOA	Testing results					Deviation
135	132	134	135	137	134	1.3
90.0	92.5	82.9	88.3	89.9	88.7	2.5
45.0	42.9	47.2	52.4	41.6	46.6	3.3
0.0	-5.2	-11.2	-11.0	-6.6	-2.2	7.2
-45.0	-37.7	-34.8	-41.8	-40.8	-39.4	6.1
-90.0	-88.4	-91.1	-84.5	-91.3	-80.2	3.9
-135.0	-135.9	-130.5	-140.6	-133.8	-141.4	3.7
-180.0	-177.1	168.5	-171.6	-177.0	169.1	7.4

Table 7.4: Testing results in real-time system for normal speech signal

Table 7.4 shows the testing results of the coherent UCA-ESPRIT algorithm when normal speech is applied. The standard deviation between the testing results and the real DOAs are with 10°. The average value of the standard deviations is 4.4°. This proves the coherent UCA-ESPRIT works properly for the real-time.

Chapter 8

Conclusion and Future works

In this thesis, a DSP-based DOA detecting real-time system is implemented, which could correctly detect the 360° azimuthal angle. The UCA-ESPRIT algorithm which is developed on the Uniform Circular Array is the basic algorithm behind the system.

The classic DOA algorithm such as MUSIC, ESPRIT in the ULA can only detect the azimuth angle from $-90°$ to $90°$. MUSIC requires calculate the MUSIC spectrum for all the possible azimuthal angle and a peak search algorithm has to be implemented afterwards to find direction-of-arrival angle. Unlike MUSIC, ESPRIT is close-form DOA algorithm which doesn't need an expensive spectral search. But ESPRIT requires two identical subarrays. The mismatch between the subarrays leads to the error of the detecting results.

Similar as ULA, there are also two DOA algorithms (UCA-RB-MUSIC and UCA-ESPRIT) in UCA. Both algorithms need to transform the element-space steering vector into beamspace via phase mode excitation. Then the beamspace steering vector becomes Vandermonde-like structure. The UCA-RB-MUSIC is to calculate the MUSIC spectrum in beamspace. UCA-ESPRIT is using the properties of the Bessel function to extract the angle directly. The phase mode excitation reduces the length of the element and only the real-part of the beamspace covariance matrix is taken into calculation. These factors make the speed of the UCA-ESPRIT faster.

The classic UCA-ESPRIT can only detect the DOA of the narrowband signals. To successfully localize the speaker, the wideband DOA algorithm has to be implemented. Here, a coherent wideband DOA algorithm is created. Unlike incoherent method, coherent method requires to calculate the narrowband DOA algorithm only once. Only the assumption has to be fulfilled that the speaker has to be far from the microphone array, which make the elevation angle approximately equal to 90°.

The test is done in a noisy room. The results shows that the deviation for detecting the narrowband signal sources is less than 10°. The error for localize the wideband signal (normal speech signal) is even less. Both show that the system could have a good performance to detect azimuthal angle.

8.1 Improvement and Future work

In the real time, the signals arrived at each microphone are attenuated with different levels. The system calculates the power of the sampled signal at each microphone to get the gain ratio to realize the amplitude calibration. This approach is the easiest but requires a lot resources to calculate, which slows down the system. To solve the problem, a AGC (Automatic Again Control) application could be developed to replace.

In this project, the DSP-board could only tape eight channel simultaneously. Therefore, the Uniform Circular Array is formed with only eight microphones. In the future, the application could be realized on a UCA with more microphones, which could improve the detecting results.

The detecting error is caused by a lot of reasons. Perhaps the noise in the room is not white enough, which distorted the signal at the selected frequencies. Or the microphone array is not well constructed. To solve these problems, an adaptive filter could be applied to attenuate the noise and an array shape calibration could be developed to compensate the imperfection of the UCA. Both of them require a lot of the computation load and will affect the speed of the real time application. It is

always a trade-off between the speed and accuracy.

Bibliography

[1] R. A. Monzingo and T. W. Miller, Introduction to Adaptive Arrays. New York: Wiley, 1980.

[2] S.U. Pillai. Array Signal Processing. Springer-Verlag, New York, 1989.

[3] S.S. Haykin. Array Signal Processing, chapter 4. S.S. Haykin Ed., Prentice- Hall, New Jersey, 1985.

[4] R.O. Schmidt. Multiple emitter location and signal parameter estimation. IEEE Trans. Antennas Propagat., 34(3):276-280, March 1986.

[5] R. Roy and T. Kailath. ESPRIT-Estimation of signal parameters via rotational invariance techniques. IEEE Trans. Acoust., Speech, Signal Processing, 37(7):984-995, July 1989. IEEE Trans. Antennas Propagat., 34(3):276-280, March 1986.

[6] Master Thesis (Wideband Audio Source Localization using Microphone Array and MUSIC Algorithm), Anshul Kant Saxena

[7] Diplomarbeit (DSP-basiertes Echtzeitsystem zur Sprecherlokalisierung mittels Mikrofonarray und Root-MUSIC), Kolja Pikora

[8] Balanis, C. A., Antenna Theory: Analysis and Design, 3rd ed., New York: Wiley, 2005.

[9] J. Yang and M. Kaveh, Adaptive eigensubspace algorithms for direction or frequency estimation and tracking, IEEE Transactions on Acoustics, Speech, Signal Processing, vol. 36, pp. 241C251, Feb. 1988. doi:10.1109/29.1516

[10] H. Krim and M. Viberg, Two decades of array signal processing research: the parametric approach, IEEE Signal Processing Magazine, vol. 13, pp. 67C94, July 1996. doi:10.1109/79.526899

[11] L. C. Godara, Application of antenna arrays to mobile communications. Part II: Beamforming and direction of arrival considerations, Proceedings of the IEEE, vol. 85, pp. 1195C 1245, Aug. 1997. doi:10.1109/5.622504

[12] T. S. Rappaport and J. C. Liberti Jr., Smart Antennas for Wireless Communications: IS-95 and Third Generation CDMA Applications, Upper Saddle River, NJ: Prentice Hall, 1999.

[13] D. E. N. Davies, Circular arrays, Chap. 12, The Handbook of antenna design, London Peregrinus on behalf of the IEE, 1983.

[14] D. E. N. Davies, A transformation between the phasing techniques required for linear and circular aerial arrays, Proc. IEE, Vol. 112, No. 11, Nov 1965.

[15] C. P. Mathews, M. D. Zoltowski, Eigenstructure techniques for 2-D angle estimation with uniform circular arrays, IEEE Trans. Signal Proc., Vol. 42, No. 9, Sept 1994, pp. 2395-2407.

[16] Master-Thesis (DSP-Based Acoustic Source Localization, Master-Thesis, 2004), Mrs Bing Li and Mrs Yuan Cheng

[17] Texas Instruments, "TMS320C67xDSP Library", Programmer's Reference Guide, SPRU657B, March 2006

[18] Chandran, S., and M. K. Ibrahim, DOA Estimation of Wide-Band Signals Based on Time-Frequency Analysis, IEEE J. of Oceanic Engineering, Vol. 24, No. 1, January 1999, pp. 116C121.

[19] Wax, M., and T. Kailath, Spatio-Temporal Spectral Analysis by Eigen-Structure Methods, IEEE Trans. on Acoustics, Speech, and Signal Processing, Vol. ASSP-32, No. 4, August 1984, pp. 817C827.

[20] Wang, H., and M. Kaveh, Coherent Signal-Subspace Processing for the Detection and Estimation of Angles of Arrival of Multiple Wide-Band Sources, IEEE Trans. on Acoustics, Speech, and Signal Processing, Vol. ASSP-33, August 1985, pp. 823C831.

[21] Fabrizio Sellone, Robust auto-focusing wideband DOA estimation, Signal Processing., vol.86, pp.17-37, .2006.

[22] PROF. DR. KOElZER and PROF. DR. SAUVAGERD, Digital Signal Processing, chap. Efficient structures for Sample Rate Converters (SRCs)